CHAPTER 7

Patterned Superhydrophobic Surfaces

ERICA UEDA[a] AND PAVEL A. LEVKIN*[a,b]

[a]Institute of Toxicology and Genetics, Karlsruhe Institute of Technology, Postfach 3640, 76021 Karlsruhe, Germany; [b]Department of Applied Physical Chemistry, Heidelberg University, Postfach 10 57 60, 69047 Heidelberg, Germany
*E-mail: levkin@kit.edu

7.1 Introduction

In this chapter, we review the fabrication and application of patterned superhydrophobic surfaces developed in recent years. We focus on how the properties and functionalities arising from patterns of superhydrophobicity combined with other surface properties, such as superhydrophilicity, on a substrate can be utilized for a range of diverse and interesting applications. The typical methods for creating uniform superhydrophobic surfaces are not always applicable for creating surfaces with patterns of wettability due to the complexity arising from the need to spatially impart different chemistry or morphology in specific locations on the surface.

The development of surfaces with patterns of wettability is being actively explored and various practical applications have already been realized, often through inspiration from nature, with the potential for many more. Nature has designed surfaces with patterns of varying wettability that are important, for example, for the survival of insects and plants. Desert beetles have

RSC Soft Matter No. 5
Non-wettable Surfaces: Theory, Preparation, and Applications
Edited by Robin H. A. Ras and Abraham Marmur

Published by the Royal Society of Chemistry, www.rsc.org

both wettable and non-wettable regions on their backs. They collect water from fog by nucleation on the non-waxy hydrophilic peaks until the water droplet grows to a critical size and then rolls down the waxy hydrophobic bumps.[1] Many groups have fabricated patterned superhydrophobic surfaces to try to mimic the beetle's ability to capture water from humid air.[2–6] The carnivorous *Nepenthes* pitcher plant also has regions of hydrophilicity and hydrophobicity to help it capture its prey.[7] The unique slippery, liquid, and self-restoring nature of the inside surface of the *Nepenthes* pitcher plant has inspired a relatively new class of surfaces termed slippery liquid-infused porous surfaces (SLIPS) that have already been developed for diverse applications such as anti-biofouling and anti-icing.[8]

These examples of wettable, non-wettable, and patterned surfaces that occur in nature can inspire new surface designs for real-world applications. In this chapter, we focus on some of the practical advantages that arise from the difference in wettability between wettable and non-wettable regions patterned on a surface: (A) wettability patterns can form surface tension-confined microchannels; (B) superhydrophobic regions in a Cassie–Baxter state can control bioadhesion on surfaces; (C) discontinuous dewetting can passively dispense aqueous solutions into wettable regions surrounded by a non-wettable background; (D) the shape and positioning of liquid droplets, particles, or microchips can be easily controlled; and (E) droplets of liquid can be efficiently collected by directing the flow of droplets. Recent methods for creating surfaces with patterns of wettability and their specific applications are discussed.

7.2 Fabrication of Surfaces with Patterned Wettability

A variety of methods are available to fabricate or tune the chemistry and morphology of surfaces to produce various wettability characteristics. However, creating surfaces patterned with combinations of extreme wetting properties, such as superhydrophilicity and superhydrophobicity, that are robust, stable, and relatively easy to fabricate is still challenging and being actively explored. In this section, we present some of the methods used to create surfaces with patterned wettability.

7.2.1 UV Light Irradiation

Takai and coworkers fabricated patterned surfaces by exposing superhydrophobic surfaces to UV light to transform the treated regions to superhydrophilic.[9] Superhydrophobic films were deposited on glass plates or Si wafers by microwave plasma-enhanced chemical vapour deposition (CVD) of a trimethylmethoxysilane and Ar gas mixture. Then, UV light with a wavelength of 172 nm was irradiated on the substrate for 30 min through a photomask to decompose the methyl groups to create superhydrophilic regions.

The process resulted in an irregular surface topography composed of granular particles and nanoscale pores on the order of a few hundred nanometers in diameter, which contributed to the superhydrophobicity. The static (θ_{st}), advancing (θ_{adv}), and receding (θ_{rec}) water contact angles of the superhydrophobic surface were 155°, 157°, and 153°, respectively. The θ_{st} of the superhydrophilic surface was 0°.

7.2.2 Phase Separation and UVO Irradiation

Mano and coworkers used a phase separation method to transform smooth hydrophobic polystyrene (PS) surfaces to rough superhydrophobic surfaces, followed by UV/ozone (UVO) irradiation to create superhydrophilic patterns on the surface.[10–13] The detailed procedure described here is from Oliveira *et al.*[11] A solution of PS (70 mg ml^{-1}) in tetrahydrofuran (THF) was prepared, and then ethanol (100% v/v) was added to the PS/THF solution at a ratio of 1.35 : 2 (v/v). A few drops of this mixture were applied to smooth PS surfaces of 0.25 mm thickness for 5 s, after which the excess mixture was removed and the substrate immersed in ethanol. The substrates were dried at room temperature, and the resulting random nano- and microstructures created an average surface roughness of 13 μm and transformed the surface to superhydrophobic. The rough PS surfaces had a θ_{st} of 151°. To create superhydrophilic–superhydrophobic patterned surfaces, the rough superhydrophobic PS surfaces were modified by UVO irradiation through a hollowed mask for 18 min to create superhydrophilic regions with a θ_{st} of 0°.

7.2.3 Hydrophilic–Superhydrophobic Black Silicon Patterned Surfaces

Chang and coworkers used single-side-polished silicon wafers as substrates to fabricate patterned hydrophilic–superhydrophobic surfaces.[14] First, 700 nm of silicon dioxide (silica) hard mask material was deposited onto the silicon wafer using plasma-enhanced CVD, and then standard photolithography with positive tone resist was used to spin and pattern a photoresist (AZ5214E) on top of the silica layer. The photoresist served as a mask for the hydrophilic sites while the unmasked silica was etched in buffered hydrofluoric acid, and then the photoresist was removed in an acetone bath. Next, black silicon was formed by the method of cryogenic inductively coupled plasma (SF_6/O_2) reactive ion etching and consisted of a random array of vertical nanospikes that contribute to the antireflective properties of black silicon.[15] Lastly, a thin layer (~50 nm) of a low surface energy fluoropolymer was deposited using CHF_3 in a reactive ion etcher, and was then lifted off from the hydrophilic sites in buffered hydrofluoric acid. This method resulted in hydrophilic sites patterned on a superhydrophobic black silicon surface.

7.2.4 UV-Initiated Free Radical Polymerization and Photografting

Polymer substrates are advantageous because of the diversity in chemical composition, surface and bulk properties, and processing techniques that are possible.[16,17] Photoinitiated polymerization and grafting allows precise control over where porous polymers, or monoliths, are formed and where surface modification takes place by irradiating specific locations with UV or visible light.

Methods based on UV-initiated free radical polymerization and surface grafting have been used to create superhydrophilic and superhydrophobic porous polymer films using different monomers and porogen ratios to control the bulk chemistry, morphology, and porosity.[18–27] The polymerization mixtures contained monovinyl and divinyl monomers, initiator, and a mixture of porogens that were required to generate porosity and surface roughness. The porous structures and globules introduced both micro- and nanoscale roughness to the material and could be easily tuned, without changing the chemistry, by changing the porogens while keeping the monomer content the same in the polymerization mixture.

Levkin *et al.* introduced a method to produce superhydrophobic porous polymer films based on UV- and thermo-initiated polymerization of alkyl methacrylates.[18] Han *et al.* and Zahner *et al.* polymerized a thin film of microporous (1–4 μm pore size) superhydrophobic or nanoporous (100–200 nm pore size) hydrophobic butyl methacrylate crosslinked with ethylene dimethacrylate (BMA-EDMA) and then modified it with a hydrophilic monomer by UV-initiated photografting through a photomask to create superhydrophilic micropatterns.[19,20] Positively charged, negatively charged, or neutral functionality could be introduced into the superhydrophilic micropatterns.[20] It is important to note that photografting occurred through the whole thickness of the porous polymer matrix resulting in the formation of three-dimensional, superhydrophilic, surface tension-confined microchannels.

Auad *et al.* used the attributes of this BMA-EDMA polymer film (the porous structure and the whole-thickness modification) to develop a simple method to rapidly create multiple superhydrophilic–superhydrophobic patterned substrates from a single template.[24] Each time adhesive tape was pressed onto the surface of a 125 μm thick BMA-EDMA polymer film and then peeled off, a thin layer of the patterned polymer was transferred to the tape and could be used as a patterned substrate. This method allowed up to 12 copies to be produced from one polymer film, thereby saving significant time and expense in creating patterned substrates.

As an alternative approach to making superhydrophilic–superhydrophobic patterned polymer surfaces, Geyer *et al.*, Ueda *et al.*, and Efremov *et al.* first prepared 12.5 μm thin, nanoporous, superhydrophilic poly(2-hydroxyethyl methacrylate-*co*-ethylene dimethacrylate) (HEMA-EDMA) polymer films by UV-initiated free radical polymerization, which were then modified with 2,2,3,3,3-pentafluoropropyl methacrylate (PFPMA) by UV-initiated

photografting through a quartz photomask to create superhydrophobic micropatterns with defined geometries (Figure 7.1).[21–23,25,27] This method is fast, flexible with respect to the monomers that can be used, and enables large areas to be patterned at once.

7.2.5 Surface Patterning *Via* Thiol-yne Click Chemistry

Photoinitiated click reactions have also been actively investigated for creating patterned surfaces due to their excellent spatial and temporal control over photochemical processes. Thiol-yne reactions are particularly advantageous because they can proceed efficiently and rapidly at room temperature and in the presence of oxygen or water, they do not require expensive or toxic catalysts, and they are compatible with a wide range of functional groups.

Patton and coworkers used thiol-yne chemistry in conjunction with UV lithography to create hydrophilic–hydrophobic patterned surfaces.[28] Poly(propargyl methacrylate) brushes with "yne" functionalities were

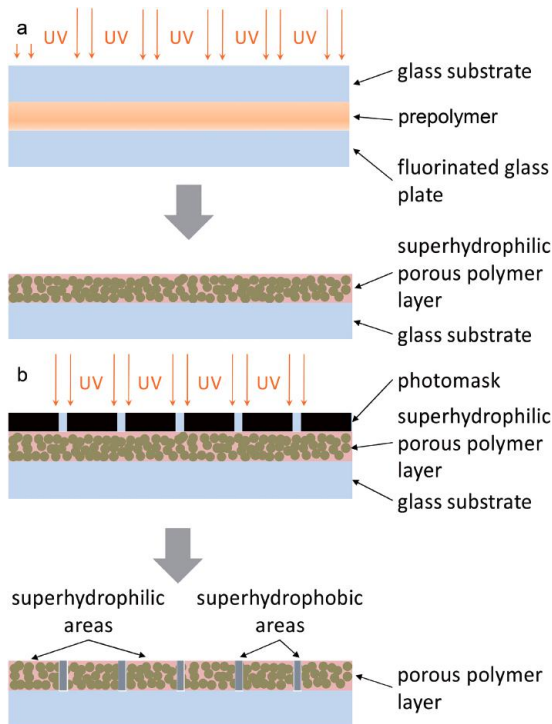

Figure 7.1 (a) Schematic of the fabrication of a superhydrophilic porous polymer film on a glass substrate by UV-initiated free radical polymerization. (b) Schematic of the fabrication of a superhydrophobic grid-like pattern on the superhydrophilic surface by UV-initiated photografting. Adapted with permission from John Wiley and Sons ref. 21. Copyright © 2011 Wiley-VCH Verlag GmbH & Co. KGaA, Weinheim.

produced *via* surface-initiated photopolymerization and subsequently functionalized with commercially available thiols.

Feng *et al.* also demonstrated the use of UV-induced sequential thiol-yne click chemistry, but as an extremely fast and initiator-free approach to create superhydrophilic–superhydrophobic micropatterns (Figure 7.2).[29] Since the thiol-yne reaction could also be performed at room temperature in water, this method was able to produce surfaces patterned with peptides as well as a variety of reactive functional groups containing a terminal thiol (*e.g.* OH, NH_2, or COOH). First, a 12.5 μm thin, porous (50% porosity, 80–250 nm pores) polymer layer of poly(2-hydroxyethyl methacrylate-*co*-ethylene dimethacrylate) (HEMA-EDMA) was prepared on a glass substrate.[21] Second, the HEMA-EDMA layer was modified with 4-pentynoic acid through a standard esterification procedure to create an intermediate, reactive alkyne surface. The resulting porous polymer bearing alkyne groups was then functionalized *via* thiol-yne click reactions initiated by irradiation with 260 nm UV light (12 mW cm^{-2}) at room temperature to transform the surface to either superhydrophobic or superhydrophilic, depending on whether hydrophobic or hydrophilic thiols were used. The reaction proceeded extremely fast, requiring only 0.5 s of UV irradiation in the presence of an initiator (2,2-dimethoxy-2-phenylacetophenone) and only 5 s without any initiator; no reaction occurred without UV light. Functionalization of the alkyne surface with cysteamine transformed the hydrophobic alkyne polymer (θ_{st} = 124°) into a superhydrophilic surface (θ_{st} = 4.4°), whereas modification with 1-dodecanethiol or 1*H*,1*H*,2*H*,2*H*-perfluorodecanethiol resulted in a superhydrophobic surface with θ_{adv}, θ_{st}, and θ_{rec} measured to be 171°, 169°, and 162° or 173°, 170°, and 164°, respectively. The porous structure of the HEMA-EDMA polymer layer resulted in a rough surface, which was proved to be an important feature for fabricating the superhydrophilic or superhydrophobic surfaces.

To create a surface with patterned wettability, the reactive alkyne surface was first modified with 5% (v/v) 1*H*,1*H*,2*H*,2*H*-perfluorodecanethiol in acetone in specific areas by irradiation with UV light through a photomask. After rinsing the substrate with acetone, the remaining non-irradiated, unmodified, reactive alkyne groups were subject to a thiol-yne reaction with 15 wt% cysteamine hydrochloride in an ethanol–water solution (1 : 1) without the need for a photomask during UV irradiation. This resulted in a surface patterned with both superhydrophilic and superhydrophobic properties, and pattern sizes as small as 10 μm could be produced.

Simply substituting the thiols with those of other functionalities during the sequential thiol-yne reactions can produce surfaces patterned with different chemistries. Since functionalization of the alkyne surface could be performed without an initiator in either apolar or polar solvents, including water, this allowed compatibility of the method with thiol-containing biomolecules, such as proteins or peptides. This was demonstrated by patterning a peptide containing a terminal cysteine residue (fluorescein-β-Ala-GGGGC) on the reactive alkyne-functionalized surface.

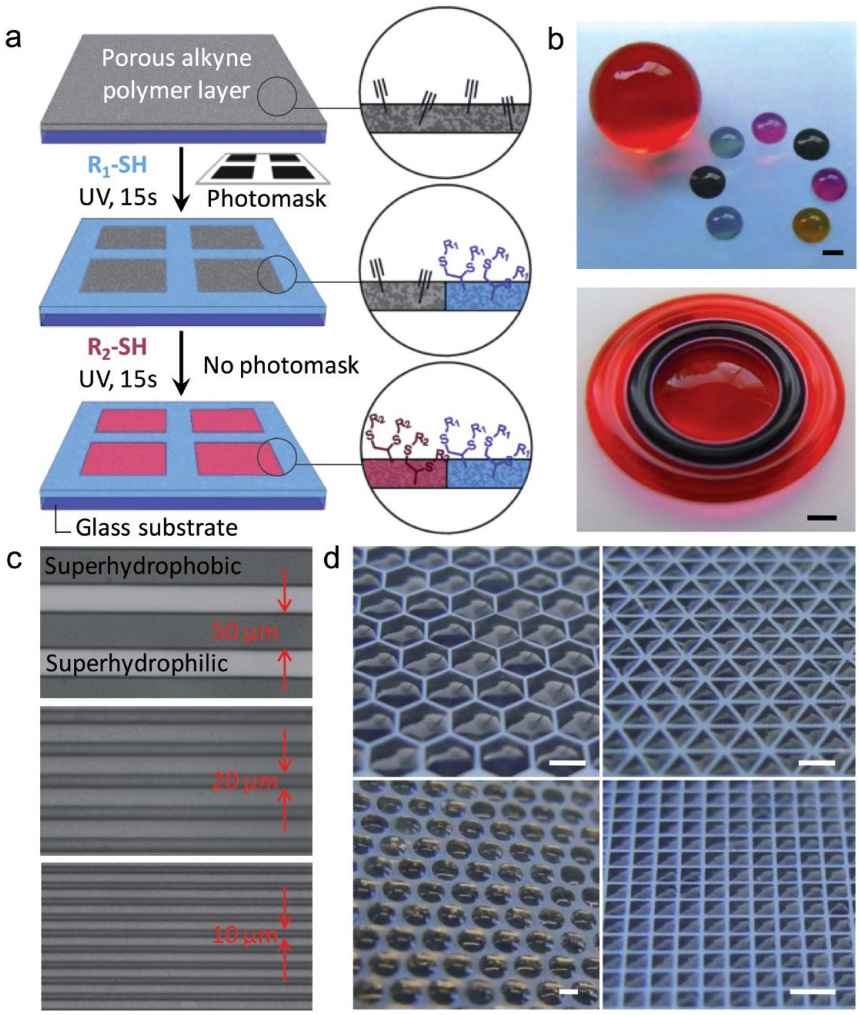

Figure 7.2 Fabrication of superhydrophilic–superhydrophobic patterns *via* thiol-yne photo–click reactions. (a) Schematic representation of the thiol-yne photo–click reaction for creating superhydrophobic–superhydrophilic micropatterns using an alkyne-modified porous polymer layer as a substrate. Optical images of (b) superhydrophilic–superhydrophobic patterns filled with dye–water solutions; superhydrophobic gap between the two rings is 100 μm. (c) Superhydrophilic regions (light areas) separated by superhydrophobic gaps (dark areas) of different widths. (d) Droplet-Microarrays formed by dipping the superhydrophobic–superhydrophilic arrays with different geometries into water. Wetted parts become transparent (dark). Scale bars are 1 mm. Reproduced with permission from John Wiley and Sons ref. 29 Copyright © 2014 Wiley-VCH Verlag GmbH & Co. KGaA, Weinheim.

7.2.6 Surface Functionalization *Via* Thiol-ene Reaction

Li *et al.* introduced a surface modification method based on creating a superhydrophobic surface with reactive vinyl groups functionalized with either molecules bearing thiol groups through a UV-triggered thiol-ene reaction or with molecules bearing disulfide groups through a UV-triggered disulfide-ene reaction.[30] They hypothesized that disulfides could react with alkenes in a similar way that thiols react with alkenes under UV light since sulfenyl radicals can be produced from disulfides upon UV irradiation. First, trichlorovinylsilane was polycondensed on a glass substrate to create thin, transparent, porous silicone nanofilaments (~30–50 nm in diameter) bearing reactive vinyl groups that formed a photoactive, inscribable, non-wettable, and transparent surface (PAINTS). Although no fluoro-containing functionalities were present, the PAINTS was superhydrophobic with θ_{st} = 166° and a water contact angle hysteresis of ~2°. High surface roughness of the silicone filaments as well as the porosity of the bulk nanofilament film probably contributed to the superhydrophobicity. This method allowed PAINTS to be easily fabricated on 3D glass objects of complex shapes, such as the inside of a glass vial and the convex side of a watch glass, without compromising their transparency.

Both the thiol-ene and disulfide-ene reactions were used to modify PAINTS to create superhydrophobic–hydrophilic patterned surfaces. To demonstrate modification using the thiol-ene reaction, a PAINTS-coated glass slide was wetted with a 10% (v/v) cysteamine in ethanol solution and irradiated with 260 nm UV light (~9 mW cm^{-2}) for 15 s. This transformed the superhydrophobic PAINTS into a highly hydrophilic surface possessing a θ_{st} of ~6°. If the UV irradiation was done through a photomask, only the irradiated regions on the PAINTS became highly hydrophilic. The non-irradiated regions still possessed reactive vinyl groups that were then modified through another thiol-ene reaction using 1*H*,1*H*,2*H*,2*H*-perfluorodecanethiol to create a superhydrophobic–hydrophilic patterned surface.

For modification through the disulfide-ene reaction, the PAINTS was wetted with a 10% (v/v) 3,3-dithiodipropionic acid in ethanol solution and irradiated with 260 nm UV light for 3 min. Again, the superhydrophobic PAINTS was transformed into a highly hydrophilic surface with a θ_{st} of ~5.1°. If a photomask covered the PAINTS during UV irradiation, then a highly hydrophilic micropattern was formed on the superhydrophobic PAINTS.

7.2.7 Surface Functionalization *Via* UV-Induced Tetrazole–Thiol Reaction

Feng *et al.* introduced a versatile UV-induced, tetrazole–thiol reaction that can be used for rapid catalyst-free polymer–polymer conjugation, efficient surface functionalization and patterning, and the functionalization of (bio) molecules bearing periphery thiol groups.[31] The method is based on 1,3-dipolar nucleophilic addition of thiols to tetrazoles, which when induced by

UV light allows the reaction to proceed rapidly at room temperature without a catalyst, with high yields, and in both polar protic and aprotic solvents. Superhydrophobic–hydrophilic micropatterns were created using this method by sequentially modifying a tetrazole-functionalized porous polymer surface with hydrophobic and hydrophilic thiols.

First, a 12.5 μm thin, hydrophilic porous polymer film composed of poly(2-hydroxyethyl methacrylate-*co*-ethylene dimethacrylate) (HEMA-EDMA) was created on a glass substrate.[21] Second, esterification of the hydroxyl groups on the HEMA-EDMA surface by 4-(2-phenyl-2*H*-tetrazol-5-yl) benzoic acid was carried out to transform the hydrophilic HEMA-EDMA surface (θ_{st} = 5°) into a hydrophobic tetrazole surface (θ_{st} = 115°). Then, sequential modifications of the tetrazole surface through UV-induced tetrazole–thiol reactions were used to create patterns of wettability on the surface. The surface was site-selectively modified with a 20% (v/v) 1*H*,1*H*,2*H*,2*H*-perfluorodecanethiol in ethyl acetate solution by irradiation with 260 nm UV light (5 mW cm^{-2}) through a photomask for 2 min, and then subsequently modified with a 20 wt% cysteamine hydrochloride in 1 : 1 ethanol–water solution under UV irradiation without a photomask. Regions of the surface modified with 1*H*,1*H*,2*H*,2*H*-perfluorodecanethiol exhibited superhydrophobicity with θ_{st}, θ_{adv}, and θ_{rec} as high as 167°, 170°, and 161°, respectively, whereas regions modified with cysteamine hydrochloride transformed the hydrophobic tetrazole surface to hydrophilic (θ_{st} = 22°). Patterns with feature sizes as small as 10 μm were feasible using this method.

7.2.8 Surface Modification Through Polydopamine

In recent years, a novel, relatively simple, and versatile method for surface modification inspired by the adhesive ability of mussels has been actively researched and developed since it was first introduced by Messersmith, Lee and coworkers.[32] Small molecules containing catecholamine functional groups, such as dopamine, are used as structural mimics of 3,4-dihydroxy-L-phenylalanine, a critical molecule found in adhesive proteins produced by mussels, and *in situ* oxidative polymerization of dopamine into a thin layer of polydopamine (PDA) is used to coat and subsequently immobilize molecules on surfaces.[33,34] PDA can be coated onto a wide variety of substrates such as ceramics, glass, metals, oxides, polymers, and silica. Surfaces can be functionalized in one step by simply coating the surface with a mixture of dopamine and the molecules to be immobilized at alkaline pH.[35–38] Polymerization of dopamine can also be controlled by exposure to UV light, even in acidic and neutral conditions, which also allows micropatterns of polydopamine to be created.[39] Further insight into applications of PDA is provided in several in-depth reviews.[40,41]

Lee and coworkers used oxidative self-polymerization of dopamine to transform superhydrophobic to hydrophilic surfaces, and created patterned surfaces by partially exposing the surface to a dopamine solution for 18 h through micromoulded capillaries.[42] The superhydrophobic surfaces were

created by coating anodic aluminium oxide (AAO) membranes with fluorosilane by gas-phase deposition. When the superhydrophobic AAO surfaces were immersed in a dopamine solution for 18 h, the surfaces changed from superhydrophobic to hydrophilic with a decrease in θ_{st} from 158.5 ± 2.8° to 37.3 ± 2.6°. To fabricate superhydrophobic–hydrophilic patterned surfaces, an alkaline dopamine solution (2 mg ml^{-1}) was injected into the microchannels and incubated for 18 h to create hydrophilic line patterns 50 μm wide.

Wang and coworkers introduced a mask-free method for creating well-defined, superhydrophilic micropatterns on a superhydrophobic surface based on the use of a piezoelectric-based inkjet printer to dispense picolitre drops of dopamine solution directly onto the superhydrophobic surface, followed by *in situ* polymerization of dopamine to PDA.[43] The dopamine solution was optimized to achieve a Wenzel wetting state to maximize interaction between the dopamine and rough superhydrophobic surface, while also having a high contact angle to precisely control the deposition of the droplet of dopamine solution on the superhydrophobic surface. In addition, to allow enough time for the oxidative self-polymerization of dopamine to take place, the surface tension as well as the vapour pressure of the aqueous dopamine droplets was reduced by adding water-miscible solvents with low surface tension (*e.g.* ethanol) or low vapour pressure (*e.g.* ethylene glycol) to induce a transition from a Cassie to a Wenzel wetting state and to prolong the time available for polymerization before evaporation of the droplet.

The superhydrophobic substrates were fabricated by spin-coating silica nanoparticles and PS granules (1–2 mm, MW 350 000) onto precleaned glass slides, calcination to fuse the silica nanoparticles together, and then coating with a semifluorinated silane of 1*H*,1*H*,2*H*,2*H*-perfluorooctyltriethoxysilane by CVD. The superhydrophobic surface exhibited θ_{st} of approximately 157° and a sliding angle of <1°. To create the superhydrophilic micropatterns on the superhydrophobic surface, the printer cartridge was filled with a freshly prepared dopamine solution (5.0 mg ml^{-1}) in a mixture of water, ethanol, and ethylene glycol (1 : 1 : 1, v/v/v), and then the inkjet printer dispensed 10 pL droplets of the dopamine solution in predesigned patterns onto the superhydrophobic substrate at room temperature. The substrate was then stored in a sealed chamber at 50 °C for 36 h to allow the dopamine to polymerize. The thickness of the PDA coating was ~45 nm and exhibited a θ_{st} of 0°. The smallest achievable feature size of the printed pattern was ~50 μm. The PDA patterns were stable for at least 1 year under ambient conditions, and could withstand flushing with water as well as with organic solvents such as acetone and ethanol.

7.2.9 Superomniphobic–Superomniphilic Patterned Surfaces

Tuteja and coworkers developed superomniphobic–superomniphilic patterned surfaces that were compatible with aqueous as well as non-aqueous, low surface tension liquids such as oil and alcohol.[44] Superomniphobic surfaces are characterized as both superhydrophobic and superoleophobic,

and similarly superomniphilic surfaces are characterized as both superhydrophilic and superoleophilic. Superomniphobic surfaces were fabricated by electrospinning solutions of 50 wt% 1*H*,1*H*,2*H*,2*H*-heptadecafluorodecyl polyhedral oligomeric silsequioxane (fluorodecyl POSS) and poly(methyl methacrylate) (PMMA). Superomniphobicity was achieved due to the highly porous, re-entrant, bead morphology of the electrospun surfaces and the low surface energy of the fluorodecyl POSS–PMMA blend. With both water and heptane, the surfaces exhibited $\theta_{adv} = 162°$ and low contact angle hysteresis $\Delta\theta = 2°$. Superomniphilic surfaces ($\theta_{adv} = \theta_{rec} \approx 0°$ for water and heptane) were obtained by exposing the superomniphobic surfaces to O_2 plasma, which most likely led to oxygen enrichment and simultaneous degradation of the fluorinated end groups in fluorodecyl POSS. Exposing the superomniphobic surface to O_2 plasma treatment through a photomask resulted in patterned surfaces with superomniphilic regions on a superomniphobic background.

7.2.10 Amine-Reactive Modification of Superhydrophobic Polymers

Lynn and coworkers presented a rapid and simple modification method based on printing an amine-containing "ink" on a superhydrophobic polymer layer to form superhydrophilic patterns.[45] The amine groups in the ink covalently attached to the amine-reactive azlactone groups of the superhydrophobic polymer, which was fabricated by layer-by-layer assembly of poly(ethyleneimine) (PEI) and poly(2-vinyl-4,4-dimethylazlactone) (PVDMA). Azlactone groups can rapidly react with primary amines through ring–opening reactions in the absence of catalysts and without the generation of by-products. The superhydrophobic PEI/PVDMA multilayers were modified through the whole thickness of the multilayer by D-glucamine (hydrophilic amine) and subsequently by n-decylamine (hydrophobic amine). First, a poly(dimethylsiloxane) (PDMS) stamp was used to contact print superhydrophilic glucamine spots (~300 μm^2) onto the PEI/PVDMA substrates, and then the substrates were immersed in a decylamine solution for 1 h to render the non-reacted azlactone groups superhydrophobic and non-wettable. Superhydrophilic patterns could also be directly drawn on the surface using a homemade glucamine-ink pen or a glucamine-soaked thread.

7.2.11 Patterns of Reversible Wettability

The methods described so far for creating surfaces with patterns of wettability are basically irreversible. Creating patterned surfaces that can easily revert back to their unmodified state is useful for applications constantly requiring many templates or changes in design patterns, such as lithography.

Fujishima and coworkers made superhydrophilic–superhydrophobic patterned substrates using a mask-free method, which were ultimately used for offset printing.[46] A rough, anodized Al plate was coated with TiO_2, modified

with octadecylphosphonic acid (ODP) self-assembled monolayers (SAMs) (θ_{st} ≈ 154°), and patterned with UV light-resistant ink by inkjet printing, which acted as a photomask. The surface was irradiated with UV light to photocatalytically decompose the ODP SAMs not covered by ink and render the regions superhydrophilic. After the ink was removed by washing with water, a superhydrophilic–superhydrophobic patterned substrate was obtained. The whole substrate could be rendered superhydrophilic again by simply irradiating the surface with UV light for 5 h. The whole process could be repeated again from the ODP modification to generate another patterned surface.

Chi and coworkers also demonstrated that patterns of wettability on a superhydrophobic surface could be alternately generated and then erased when using an alcohol-based ink.[47] Additionally, the superhydrophobic regions could be reversibly adjusted between a sticky or sliding behaviour of droplets on the surface. An electrochemical anodizing process was used to fabricate a surface composed of vertically aligned and uniformly distributed TiO_2 nanotubes of 100 nm outer diameter and 400 nm length. Water on the TiO_2 nanotube array (TNA) film rapidly spread and wetted the surface, but after modification with 1*H*,1*H*,2*H*,2*H*-perfluorooctyltriethoxysilane the surface became superhydrophobic (θ_{st} = 160°) with water droplets exhibiting a spherical shape and low adhesion to the surface. A pen or inkjet printer was used to dispense a smooth layer of the waterproof, alcohol-based ink (surface tension in the range of 20–32 mN m^{-1}) on the surface of the superhydrophobic TNA. The smoothness of the hydrophilic ink layer reduced the surface roughness and increased the solid–liquid contact area, resulting in enhanced water adhesion and hydrophilicity (θ_{st} ≈ 82°) on the inked regions.

Superhydrophobic–superhydrophilic patterns were fabricated by taking advantage of the photocatalytic property of TiO_2 and the ability of the ink to act as a photomask to shield the underlying surface from UV light. First, a hydrophilic ink pattern was drawn with a pen on the superhydrophobic TNA film. Then the surface was irradiated with UV light, during which the fluoroalkyl groups not protected by ink were decomposed by the TiO_2 film and resulted in a wettability change from superhydrophobic to superhydrophilic. After removing the ink layer by rinsing the surface with a methanol solution, the superhydrophobic TNA surface had superhydrophilic micropatterns. Larger and complex ink patterns can be achieved by using an inkjet printer to dispense ink on the superhydrophobic TNA surface.

To adjust the superhydrophobic surface from a sliding Cassie–Baxter state to a sticky Wenzel state, a micro-sized ink layer was created on the superhydrophobic TNA surface. Droplets were pinned on ink dots on the superhydrophobic TNA surface even at a tilt angle of 90° or 180°. To revert back to the sliding state, the alcohol-based ink was removed from the surface by simply washing the surface in a methanol solution for 30 s. Water droplets rolled off the recovered superhydrophobic TNA surface when the substrate was tilted >10°. This quick and reversible adhesion switching on the superhydrophobic TNA surface could be repeated many times by printing then erasing the ink.

Li *et al.* presented a rapid and simple method of printing an "ink", a phospholipid in ethanol solution, onto a thin, microporous, superhydrophobic polymer layer to create superhydrophilic spots within a superhydrophobic background.[48] The ink was simply dispensed on the surface and then dried under ambient conditions. The method is compatible with various printing technologies such as contact printers, dip-pen nanolithography, and inkjet printers to make high-density arrays or intricate patterns of superhydrophilic spots. Chemicals that were added to the solution of phospholipid ink printed onto the superhydrophobic surface resulted in arrays of superhydrophilic spots prefilled with chemicals. This allows easy multiplexing and patterning of deposited substances.[49]

Liu and coworkers used an atmospheric-pressure plasma jet (APPJ) to create superhydrophilic patterns on various superhydrophobic metal surfaces by decreasing the hydrophobic fluorine-containing functional groups and increasing the hydrophilic oxygen-containing functional groups on the APPJ-treated regions.[50] The APPJ (~4 mm in diameter) was generated by bare electrode discharge without the need for expensive vacuum equipment. The superhydrophobic substrates were fabricated by first electrochemically treating polished metal plates (*e.g.* aluminium, copper, titanium, or zinc) to create roughness on the surface, and then immersing the substrates in a 1 wt% fluoroalkylsilane ($C_6F_{13}C_2H_4Si(OCH_2CH_3)_3$, FAS) in ethanol solution to fluorinate the surface and lower the surface free energy. Masks were used to selectively expose the superhydrophobic metal substrates to the APPJ to create superhydrophilic patterns such that the θ_{st} decreased from 159° to <5° after 45 s of exposure. APPJ treatment did not significantly affect the surface morphology. The superhydrophobicity of the surface could be recovered simply by immersing the substrate in the FAS–ethanol solution again for 2 min, and this reversible wettability transition could be repeated for at least five cycles.

7.3 Applications of Patterned Superhydrophobic Surfaces

In this section, we present a diverse range of applications that take advantage of the unique wetting properties of surfaces with patterned wettability. In general, these patterned surfaces are designed with wetting and non-wetting regions to control the deposition, flow, or position of liquids on surfaces, or alternatively to create bioadhesive and non-bioadhesive regions.[51]

7.3.1 Open Microfluidic Channels

Microfluidic devices are able to manipulate minute volumes of samples and thus can be used to carry out miniaturized chemical reactions and biological assays. However, external components such as pumps and valves are usually needed and add complexity to the platform. As an alternative to these microfluidic devices, the use of surface tension-confined microfluidic

(STCM) devices based on the principle of surface tension to passively control the movement of liquids, instead of pumps, is being actively developed for a variety of applications.[52] STCM devices transport small volumes of liquid along tracks that exhibit a higher surface energy compared to the background region through the use of surface tension gradients, capillary force, gravitational force, and pressure differences, without the need for pumps or physical walls along the tracks. For example, aqueous solutions can be transported along high surface energy, hydrophilic 2D channels while the surrounding hydrophobic regions act as virtual walls that contain the liquid along the hydrophilic path.

Fréchet and coworkers photopatterned a superhydrophilic channel in a superhydrophobic, porous polymer layer and used the channel to separate peptides of different isoelectric point and hydrophobicity by 2D thin layer chromatography.[19] The separated peptides were identified by desorption electrospray ionization mass spectroscopy directly from the polymer surface, which was possible due to the open nature of the device. There is great potential for open microfluidic devices used in conjunction with a variety of detector systems in the field of miniaturized separation and diagnostics.

Hancock *et al.* used surfaces with patterns of wettability to passively generate gradients of chemicals or particles.[53,54] Hydrophobic boundaries were created on a hydrophilic glass slide simply by using tape to mask the desired hydrophilic pattern and applying a hydrophobic spray to the background. When a solution was dispensed at one end of a hydrophilic stripe or more complex shape, the difference in curvature pressure generated a flow and created a concentration gradient by convection along the hydrophilic region as the hydrophobic boundaries contained the flow. Hancock *et al.* used the hydrophilic–hydrophobic patterns to also create gradients of solutes, cells, and microspheres encapsulated in 3D hydrogels by photocrosslinking prepolymeric solutions in the hydrophilic stripes.[55,56] Lin and coworkers also created 3D hydrogels using complex, geometric hydrophilic–hydrophobic patterns, which were subsequently used as moulds to form PDMS channels.[57]

Efremov *et al.* used surfaces patterned with arrays of hydrophilic spots surrounded by hydrophobic barriers to quickly generate various customized liquid structures on the same substrate without the need for complex equipment.[27] The method, termed "digital liquid patterning", was inspired by the working principle of a digital scoreboard. Similar to lighting up specific bulbs to form a pattern on the scoreboard, specific hydrophilic spots were filled with aqueous solutions to form a pattern of drops among the array of hydrophilic spots. The individual drops in adjacent hydrophilic spots could also be made to coalesce across the hydrophobic barrier using a pipette tip to create continuous liquid patterns or channels. This method was also used to create hydrogel structures as well as patterns and gradients of silica microparticles and cells within the surface tension-confined liquid channels. An advantage of this maskless method is that the desired liquid pattern can be changed on demand simply by manual pipetting.

Lee and coworkers used STCM channels to create a gravity-driven microfluidic device to move and mix droplets.[58] The 2D channels were formed by micropatterning lines of hydrophilic polydopamine (PDA) (60 μm wide, 200–300 nm thick) on nanostructured, superhydrophobic, AAO surfaces. Gravity caused water droplets to move along the patterned PDA microlines when the patterned surface was tilted downwards by 5°. To promote the mixing of two droplets, Y-shaped PDA microlines with a square micropatch (200 μm wide) of PDA at the intersection were patterned on the superhydrophobic AAO substrate. The first water droplet (10 μl) rolling down one arm of the Y-pattern was captured on the micropatch due to surface tension, but after the second water droplet (10 μl) was released down the other arm of the Y-pattern and mixed with the first droplet, the coalesced droplets continued to move downwards. The balance between the gravitational force and the surface tension applied to the droplets on the PDA micropatch was enough to capture the first droplet, but not enough to hold both droplets after mixing. The capability of this mixing device was further demonstrated by using it to synthesize gold nanoparticles. Thus, open STCM devices have proved to be a relatively simple tool to control the movement of droplets on surfaces and can be utilized as chemical microreactors.

7.3.2 Cell Patterning and Cell Microarrays

In this section, we discuss how patterns of wettability can be used to control the adhesion of proteins, cells, bacteria, and microorganisms on surfaces. Often, a non-wettable background is used to confine solutions within the wettable regions on a surface. Similarly, a background exhibiting a superhydrophobic Cassie–Baxter state is able to confine cells within the hydrophilic regions due to the inability of cells to adhere firmly to the surface because of the limited cell–surface contact area and reduced protein adsorption.

Superhydrophobic surfaces exhibiting the Cassie–Baxter state effectively trap air in the surface asperities, preventing the penetration of aqueous solutions.[59,60] Cell–surface interactions are influenced by proteins present on the surface and those that adsorb onto the surface from the culture medium, followed by deposition of the cell's own extracellular matrix (ECM). Since only a small fraction of the superhydrophobic surface contacts the culture medium, this likely reduces the number of sites available for protein adsorption and deposition of the cell's own ECM as well as subsequent focal adhesions.[61] Even at these limited points of contact between the culture medium and the superhydrophobic surface, adsorbed proteins such as fibronectin can demonstrate alterations of the domain conformations involved in cell adhesion, and reorganization or exchange of the adsorbed proteins with those deposited by the cells can be significantly inhibited on superhydrophobic surfaces.[61,62] These events would further discourage cell adhesion on superhydrophobic surfaces.

Takai and coworkers demonstrated that the design of superhydrophilic–superhydrophobic patterns can influence cell adhesion and morphology, as

well as ECM production.[9] Mouse embryonic fibroblast (3T3) cells spontaneously recognized and migrated towards the superhydrophilic regions after being seeded on the patterned surface, and immediately adhered there and grew to confluence after 24 h. Maintenance of the cells within an array of superhydrophilic spots depended on the distance between the spots. At inter-spot distances of 150 μm, confluent cells in the superhydrophilic spots began to make contact with cells in adjacent spots. At longer inter-spot distances of 400 μm, no physical cell–cell contact occurred between cells in adjacent spots. In contrast, cells required 24–72 h after seeding to adhere to the superhydrophobic background. This difference in cell adhesion behaviour was attributed to the difference in protein adsorption on the superhydrophilic *versus* superhydrophobic regions. Since proteins adsorbed less efficiently on the superhydrophobic regions, the cells needed time to produce their own ECM to form a protein layer suitable for adhesion.

Mano and coworkers studied cell adhesion and proliferation on rough *versus* smooth hydrophobic and hydrophilic PS surfaces.[11] Human primary osteosarcoma cells (SaOs-2) adhered more on the smooth hydrophilic and rough superhydrophilic PS surfaces, and did not significantly attach or proliferate on either the smooth hydrophobic or rough superhydrophobic PS surfaces even after 6 days of culture. In contrast, mouse lung fibroblast cells (L929) reached confluence on both hydrophobic surfaces after 6 days of culture, which was attributed to the ability of fibroblasts to proliferate quickly, and specifically to the greater ability of L929 cells (compared to other cell types) to proliferate even in unfavourable culture conditions. Enhanced initial cell adhesion on the rough superhydrophilic *versus* smooth hydrophilic surface was attributed to the surface roughness, which increased the surface area available for cell–surface contacts and promoted more exposure of oxygen-rich chemical groups on the surface that can bind cells and support high cell adhesion. When superhydrophobic substrates patterned with superhydrophilic squares (1 mm side length) were immersed and cultured in medium containing SaOs-2 cells for 6 days, the superhydrophilic regions became densely populated with cells while only a few cells occupied the superhydrophobic background.

Further examples are available where superhydrophobicity is used to confine cells within (super)hydrophilic patterns on a surface. Chi and coworkers found that 3T3 cells cultured on a superhydrophobic TiO_2 nanotube array surface patterned with hydrophilic ink regions preferentially immobilized on the ink-covered hydrophilic regions and were confined in the ink patterns by the surrounding superhydrophobic region.[47] Feng *et al.* used UV-induced, sequential thiol-yne click chemistry to create superhydrophilic–superhydrophobic micropatterns.[29] Human cervical adenocarcinoma cells (HeLa-GFP) adhered well to the superhydrophilic microspots, and less than 1% of the cells occupied the superhydrophobic regions separating the microspots after 2 days of culture. Li *et al.* created superhydrophobic–hydrophilic micropatterns on a surface composed of a thin layer of silicone nanofilaments.[30] They demonstrated cell patterning on these surfaces and reported that 94% of

the human embryonic kidney cells (HEK 293) cultured on the surface after 24 h were confined within the hydrophilic squares and only 6% of the cells occupied the superhydrophobic barriers. Feng *et al.* created superhydrophobic–hydrophilic micropatterns by sequentially modifying a tetrazole-functionalized porous polymer surface with hydrophobic and hydrophilic thiols.[31] Rat mammary carcinoma cells (MTly) cultured on the patterned surfaces adhered well to the hydrophilic areas, but the superhydrophobic barriers demonstrated efficient cell repellency.

Efremov *et al.* cultured multiple cell types separately in microreservoirs formed within hydrophilic patterns on a superhydrophobic, nanoporous polymer substrate.[23] They demonstrated that hydrophilic–superhydrophobic patterned surfaces facilitated cell patterning as well as the study of cell–cell signalling processes *in vitro*. In this case, two different cell populations were initially seeded in adjacent microreservoirs and subsequently cultured in shared medium after adhesion of the cells to the surface, and then the cross-talk between the two cell populations *via* Wnt signalling molecules was monitored and analysed.

The unique properties arising from patterns of superhydrophilicity and superhydrophobicity on a surface also offer advantages in the field of cell microarrays. Cell microarrays have become a valuable tool for high-throughput screening due to their miniaturized format and the economical use of precious cells, reagents, and consumables compared with conventional microtitre plates. For example, reverse cell transfection microarrays have been developed and implemented for genetic screening to discover the role of genes in cellular processes or to identify drug targets.[63–72] Typically, oligonucleotides and transfection reagents are mixed with ECM components that promote cell adhesion, and then printed onto a surface. Cells are then seeded over the whole surface to ultimately form clusters of transfected cells within a background of non-transfected cells, or the background is passivated such that the cells mainly adhere to the spots of interest. Instead of passivating the background with surface coatings such as poly(ethylene glycol) (PEG) or albumin to prevent cell adhesion, superhydrophobicity can be used to control the patterning of liquids and cells on microarray surfaces.[73–78]

Superhydrophilic–superhydrophobic patterned surfaces offer several advantages over the conventional non-patterned glass slides that are often used for cell microarrays: higher spot density due to confinement by the superhydrophobic barriers of both the printed solutions and cells within the superhydrophilic spots; and low variation in the spot size and resulting concentration of the printed samples on the surface (independent of the properties of the aqueous solution or surface) due to confinement of the printed solutions by the superhydrophobic barriers. Typical layouts for cell microarrays have spot diameters in the range of 200–500 μm printed at a pitch of 500–1500 μm.[66,77,79–81]

Geyer *et al.* fabricated densely packed, superhydrophilic squares (335 μm side length) separated by narrow (60 μm wide), superhydrophobic barriers on a nanoporous polymer substrate to create a cell microarray with a sixfold

higher spot density compared with a non-patterned glass slide.[21] Aqueous solutions dispensed in individual superhydrophilic squares completely wetted the squares, but were completely contained by the watertight superhydrophobic barriers. MTly, HEK 293, and mouse hepatoma (Hepa) cells all preferentially adhered and grew to confluence on the superhydrophilic squares. The superhydrophobic barriers prevented cell proliferation on the barriers and cell migration between adjacent spots, which was attributed to reduced cell–surface contact due to air being trapped inside and on the surface of the rough, nanoporous, superhydrophobic barriers exhibiting the Cassie–Baxter state. This notion was further demonstrated by showing that almost no cell pattern formed when the superhydrophobic barriers were transitioned from the dry Cassie–Baxter to the wetted Wenzel state. The patterned substrates were used for reverse cell transfection experiments by dispensing a plasmid DNA transfection mixture onto the superhydrophilic squares before cell seeding. In principle, superhydrophilic–superhydrophobic patterned substrates can be used for cell screening with a variety of bioactive molecules.

Although surface chemistry can be used to control cell adhesion, its effectiveness can be highly dependent on the cell type and the composition of the culture medium as the original chemical pattern is obscured over time with adsorbed proteins. Mano and coworkers found that less protein was adsorbed on rough superhydrophobic surfaces, independent of the underlying surface chemistry, and attributed this to the Cassie–Baxter effect.[82] This also resulted in a lower affinity of cells to the rough superhydrophobic surfaces. Thus, superhydrophobicity can be used as a more general approach for controlling protein and cell adhesion since liquid–surface interactions are minimized, and using superhydrophobic barriers to confine cells can be an interesting and effective alternative to using physical barriers for applications such as cell patterning, cell microarrays, and lab-on-a-chip or diagnostic devices.

7.3.3 Cell or Chemical Screening in Arrays of Liquid or Hydrogel Droplets

Cell microarray technology is usually limited to screening adherent cells in a 2D format, and, depending on the diffusion rate of the components of the printed solutions or the factors secreted by the cells, neighbouring spots can cross-contaminate each other by diffusion of chemicals through the shared culture medium. Cell screening platforms are being developed to address these issues, such as the use of surfaces with patterned wettability to encapsulate chemicals and cells in individual droplets or hydrogels arrayed on the surface. These droplet arrays enable screening of adherent as well as non-adherent cells with chemical stimuli in a 2D or 3D microenvironment.

Mano and coworkers deposited droplets of cell suspension in hydrophilic spots patterned on a rough, superhydrophobic PS substrate and cultured the cells in the isolated droplets.[12] Aqueous solutions were confined within the

square (super)hydrophilic spots (1 mm side length) due to the large difference in surface tension compared with the superhydrophobic background. Hydrophilic spots were individually coated with different concentrations of human serum albumin and human plasma fibronectin, and then a 10 μl droplet of cell suspension was manually dispensed onto each hydrophilic spot and cultured for 4 h. In general, more cells were detected on the spots with higher amounts of human plasma fibronectin, which is cell adhesive due to the presence of integrin binding domains, whereas albumin is a passivating protein.

Mano and coworkers also performed a combinatorial screen of the chemical composition and cytocompatibility of 3D hydrogels in an array format on hydrophilic–superhydrophobic patterned substrates.[13] The hydrophilic squares (2 mm side length) were separated by 0.5 mm on a superhydrophobic PS surface. Chitosan, collagen, or hyaluronic acid was combined with alginate at different ratios to create 24 combinations of alginate-based polymers. The pre-polymer solutions were mixed with cells and then dispensed as droplets on the hydrophilic squares using a micropipette. $CaCl_2$ was added to the droplets to ionically crosslink the polymers to form hydrogels, and then the substrate was immersed in culture medium. Fibroblasts (L929) or pre-osteoblasts (MC3T3-E1) were cultured in the hydrogels for 24 h, and both non-destructive (live/dead cell staining and image analysis) and destructive (proliferation assay and dsDNA quantification) methods were used to analyse the cytocompatibility of the hydrogels. This platform demonstrates the potential of surfaces with patterned wettability to create hydrogel arrays to study cell–material or cell–molecule interactions in 3D microenvironments.

Arrays of droplets or hydrogels are typically formed by manual pipetting, but this considerably limits the scale of spots that can be made in practice, and should be replaced by a technology more suitable for high-throughput screening. Chatelain and coworkers developed the "DropChip" microarray to perform multiplexed cell-based assays in isolated droplets in a high-throughput manner.[83] The DropChip featured up to 100 nl droplets on hydrophilic spots of bare glass (500 μm diameter, 1 mm spot pitch) surrounded by a hydrophobic perfluoro-octylsilane background. A piezoelectric-controlled spotting device was used to precisely dispense droplets of cells, drugs, and nucleic acids onto the DropChip. The spots can be assayed in parallel simply by dipping the slide in solutions such as those for fixing or staining cells.

Ueda *et al.* used the concept of discontinuous dewetting on a superhydrophilic–superhydrophobic patterned surface to create high-density arrays of aqueous droplets or hydrogels encapsulating cells, without the need to manually pipette each droplet or use automated equipment.[22] The simple method relies on the large difference in wettability between the superhydrophilic and superhydrophobic regions to passively dispense thousands of isolated droplets in the superhydrophilic spots, referred to as a Droplet-Microarray. During discontinuous dewetting, the trailing edge of an aqueous solution moving along the patterned surface becomes pinned at the borders between the superhydrophilic and superhydrophobic regions due

to a sudden and extreme change in θ_{rec}, until the liquid film thins and finally breaks to form a droplet in each superhydrophilic spot.[84–87] The volume of the individually formed droplets ranged from 700 pl to 3 μl depending on the size and geometry of the superhydrophilic spots as well as on the surface tension of the solution. The Droplet-Microarray can be an alternative to growing suspension cells in microwells or in a hanging drop. Furthermore, discontinuous dewetting was used to create crosslinked maleimide–polyvinyl alcohol hydrogel micropads encapsulating cells that were immobilized within the superhydrophilic spots. After the array of hydrogels is formed, the substrate can be immersed in shared culture medium or droplets of medium can be formed in each superhydrophilic spot to isolate each hydrogel. When hydrogels encapsulating cells were incubated individually on superhydrophilic spots pre-printed with increasing amounts of doxorubicin, a cancer drug, a concentration-dependent effect on cell viability was observed. This demonstrated that chemicals printed and dried in the superhydrophilic spots were able to diffuse into the isolated hydrogels without cross-contaminating the adjacent spots. The patterned substrates could also be compatible with other published methods for forming hydrogels, such as dispensing a hydrogel precursor solution that crosslinks upon UV irradiation or forming alginate hydrogels by ionic crosslinking with the addition of calcium chloride.[13,88,89]

To address the challenge of simultaneously adding substances to each individual droplet on a Droplet-Microarray, Popova *et al.* developed a "Droplet–Array (DA) sandwich chip" that involved sandwiching a Droplet-Microarray with a substrate printed with substances in a matching array format.[90] The sandwich method is applicable for high-throughput, cell-based screenings with the possibility of (1) one-step seeding of adherent or non-adherent cells in individual droplets and culturing for at least 24 h, (2) simultaneous addition of substances into individual droplets without cross-contamination, (3) chemically treating or transfecting cells in droplets, and (4) low consumption of reagents and cells. The DA slide consisted of an array of superhydrophilic, nanoporous 2-hydroxyethyl methacrylate-*co*-ethylene dimethacrylate (HEMA-EDMA) spots (1 mm diameter) on a superhydrophobic background (Figure 7.3). Discontinuous dewetting was used to form an array of isolated microdroplets (60 nl) encapsulating cells by sliding a cell suspension down a tilted patterned substrate. A library microarray (LMA) slide was prepared by printing drugs or transfection mixtures onto a bare glass slide using a non-contact, ultralow volume dispenser in an array format corresponding to the pattern of the DA slide. Simultaneous addition of substances into each individual droplet was achieved by precisely aligning and sandwiching the DA slide with the LMA slide. The printed chemicals and transfection mixtures dissolved and diffused into the individual droplets, after which the LMA was removed and the DA was cultured in medium.

When HeLa and HEK293 cells were cultured in droplets for 24 h, both cell types showed a typical spread morphology with viability rates of 96% and 98%, respectively. The sandwiching approach was used for the parallel addition of different amounts of the drug doxorubicin printed onto a LMA

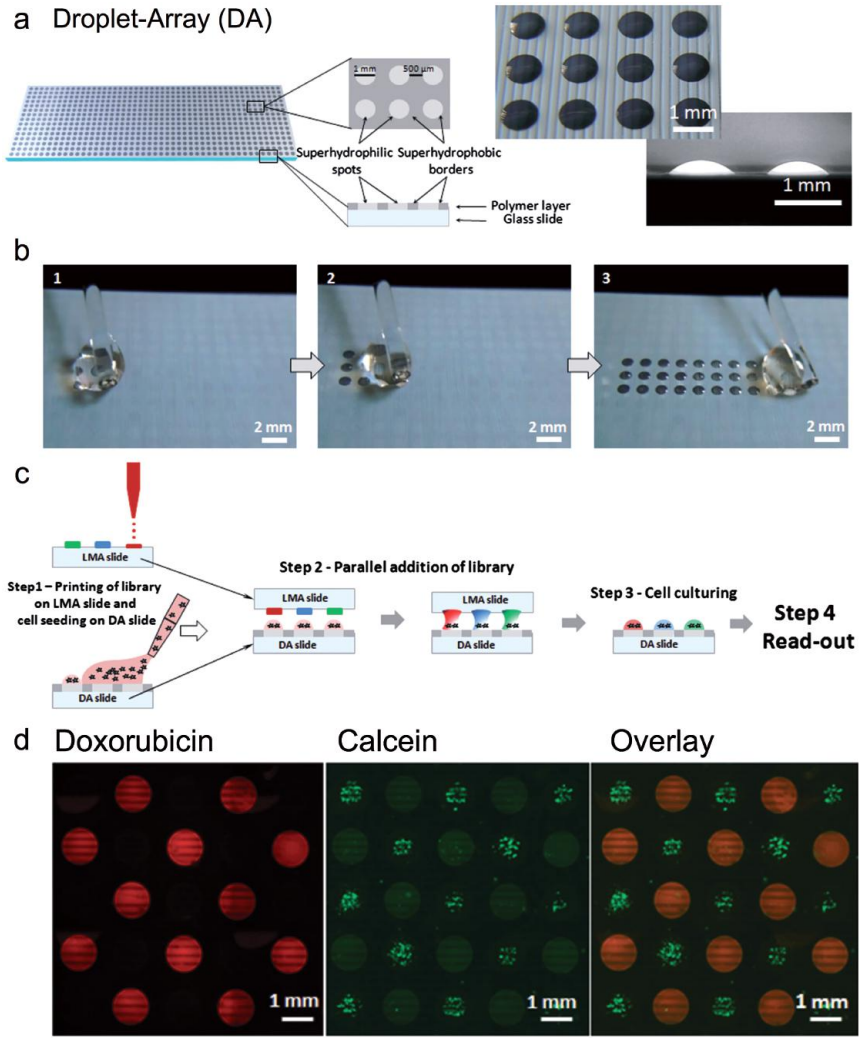

Figure 7.3 (a) Schematic of a Droplet–Array (DA) slide and images of droplets formed on a superhydrophobic–superhydrophilic pattern. (b) Snapshots of the process of discontinuous dewetting leading to the formation of an array of microdroplets. (c) Schematic of the workflow for cell-based screenings using the DA sandwich chip. Library microarray (LMA) slide is prepared by printing substances of interest on a glass slide (Step 1). DA slide is prepared by seeding cells using discontinuous dewetting (Step 1). For parallel addition of a library into individual droplets, the LMA slide is aligned and sandwiched with the DA slide containing cells (Step 2). After the substances are transferred into the droplets, the LMA slide is removed and the DA slide is placed into a cell culture incubator (Step 3). (d) Fluorescence microscopy images of a DA slide containing HeLa cells 18 h after treatment with doxorubicin. Doxorubicin shows red fluorescence (left). Calcein-stained HeLa cells on the same DA slide (middle). Overlay of the images (right). Adapted with permission from John Wiley and Sons ref. 90.

hydrophobic glass slide to a DA slide with microdroplets containing live HeLa cells. The cells in droplets sandwiched with the spots on a LMA printed with 25 ng of doxorubicin had few live cells, as indicated by Calcein staining at 18 h of culture post sandwiching (Figure 7.3). The sandwich method was also used to perform parallel gene overexpression in HEK293 cells seeded on a DA slide by sandwiching with a LMA slide arrayed with dried transfection mixtures. HEK293 cells showed a transfection efficiency of ~20%.

So far, substrates with patterns of wettability have shown potential for performing more sophisticated cell screenings than 2D cell screening platforms. Although small pattern sizes allow high-density arrays to be achieved, the limitations of working with very small droplet volumes for culturing cells are preventing droplet evaporation and nutrient starvation, especially during long culture times. Another important issue to address is how to exchange the solution in droplets, especially for those containing non-adherent cells, for processes such as medium exchange or performing assays. In principle, hydrogels can be functionalized or incorporated with ECM proteins, signalling molecules, or chemicals to enable sophisticated cell screenings in a 3D microenvironment. Culturing cells in 3D microenvironments, such as hydrogels, *versus* 2D cell culture gives the opportunity to study cells in an environment that more accurately resembles the *in vivo* situation.[88,91] In addition, the physical properties of hydrogels such as stiffness and degradability can be tuned.[92] Even plasmids can be incorporated into the hydrogels for transfection in 3D.[93] High-throughput screening of cells in 3D systems is an important tool that can provide valuable information, but the methods are still being established.

Arrays of droplets on hydrophilic–hydrophobic patterned surfaces can also be used for the synthesis and quantitative analysis of chemicals in a high-throughput manner. Balakirev and coworkers used nanodroplets positioned on a micropatterned surface to synthesize and profile new enzyme inhibitors of the NS3/4A serine protease of the hepatitis C virus (HCV), which plays an essential role in the maturation and immune evasion of HCV.[94] Nanodroplets were printed onto hydrophilic spots (500 μm diameter) patterned on a hydrophobic surface. Potent inhibitors of the NS3/4A protease were identified within a set of 200 hydrazides and 20 100 distinct dihydrazones synthesized inside the nanodroplets.

Balakirev and coworkers also used droplets on the hydrophilic–hydrophobic patterned surfaces for the synthesis and screening of 1600 unique fluorophores with a drug-like scaffold that could act as bioimaging probes.[95] The crucial role of the amidine structure for fluorescence was discovered. These examples demonstrate that droplets on patterned surfaces can be an extremely useful tool for creating combinatorial libraries and miniaturizing drug or molecular discovery efforts.

Tuteja and coworkers used superomniphobic–superomniphilic patterned surfaces such that arrays of droplets with both aqueous or non-aqueous solutions could be formed.[44] When the patterned surface was dipped in heptane, the extreme wettability contrast of the patterned surface caused heptane to selectively wet the superomniphilic regions and resulted in the self-assembly

of heptane droplets within these regions. These droplets of organic liquids have the potential to serve as microchannels or microreactors for liquid-phase reactions in the future.

Similarly, Feng *et al.* used discontinuous dewetting on patterned surfaces to create high-density arrays of microdroplets of organic liquids with surface tensions as low as 18.4 mN m^{-1}.[96] Low surface tension organic liquids wetted and formed droplets in the cysteamine micropatterns fabricated on a chloro(dimethyl)vinylsilane-coated flat glass surface, but did not wet the surrounding *1H*,*1H*,*2H*,*2H*-perfluorodecanethiol-modified areas. This approach was further used for the formation of homogeneous arrays of hydrophobic nanoparticles, polymer micropads of controlled shapes, and polymer microlens arrays. To demonstrate the potential for performing miniaturized and parallel high-throughput chemical reactions in organic solvents without multiple pipetting steps, a library microarray (LMA) slide printed with two different dyes was sandwiched on top of a slide with an array of 1-butanol microdroplets. This led to the dissolution of the chemicals in the individual microdroplets without cross-contamination between adjacent droplets. In addition, water–oil interfaces in microdroplets were formed by sandwiching an oil microdroplet array with an aqueous microdroplet array formed on a superhydrophobic–superhydrophilic pattern, which could enable miniaturized parallel liquid–liquid microextractions or heterophasic organic reactions.

7.3.4 Positioning or Sorting Particles

Fan and Stebe evaporated particle suspensions on lyophobic surfaces patterned with lyophilic regions to position and sort particles by size.[97] As the solution evaporates, the contact line recedes and fills the lyophilic features with discrete droplets by way of discontinuous dewetting. Sorting occurs by creating droplets on the lyophilic features with dimensions larger than the particles of interest and smaller than those to be excluded. For example, 210 nm amidine-functionalized PS particles could be separated from a suspension also containing 810 nm particles by evaporating the suspension on a surface patterned with 1 μm-wide stripes of wettable COOH-terminated SAMs surrounded by non-wettable CH_3-terminated SAMs on a gold-coated surface. In another example, a solution containing 900 nm and 5.46 μm PS particles functionalized with streptavidin and bound to biotinylated dye biotin-4-fluorescein or Alexa-fluor 594 biocytin, respectively, was evaporated on a surface patterned with 5 μm and 25 μm square lyophilic patches. All of the lyophilic spots contained the smaller 900 nm particles that fluoresced green, while only the 25 μm squares contained the larger 5.46 μm particles and fluoresced red. Particles could also be deposited and sorted by dip-coating the patterned surface in a solution. This method is applicable for sorting any particles that can be suspended in a solvent and the ability to create patterned lyophilic and lyophobic regions, and thus maybe be useful for creating arrays for biosensors and in microphotonics.

Vermant and coworkers used a Langmuir–Blodgett deposition technique to assemble micrometre-sized, sulfate-modified PS particles (2.9 μm diameter, 9.7 μC cm^{-2} surface charge density) from an oil–water interface onto a hydrophobic silicon substrate patterned with hydrophilic regions.[98] Decane–water was used as the fluid–fluid interface to enhance dipolar repulsion of colloids to form a highly ordered and stable monolayer at the interface during Langmuir–Blodgett deposition, which resulted in planar colloidal clusters on the hydrophilic regions where the cluster size depended on the pattern size. Particles were deposited onto square hydrophilic spots (side length = 7.5 μm or 5 μm, spacing = 5 μm or 6 μm, respectively) using the Langmuir–Blodgett technique and resulted in an average cluster size of 12.74 and 6.25 particles per cluster, respectively, with low dispersity in size. Improving self-assembly of the colloids into more complex forms by increasing the geometric complexity of the hydrophilic pattern should be further studied.

Tuteja and coworkers used superomniphobic–superomniphilic patterned surfaces for the wettability-driven self-assembly of microparticles and polymers from both aqueous solutions and liquids with low surface tension (*e.g.* heptane).[44] When the patterned surface was dipped in an aqueous or organic solution, the extreme wettability contrast of the patterned surface caused the solution to selectively wet the superomniphilic spots and resulted in the self-assembly of droplets within these spots. Dispersions of UV fluorescent green microspheres in water or UV fluorescent red microspheres in heptane became confined within the superomniphilic regions when sprayed onto patterned surfaces, demonstrating the compatibility of the surfaces with both high and low surface tension liquids. Such precise control over the site-selective, self-assembly of particles and films can be useful for fabricating electronic and optical devices, patterning cells, or forming well-defined thin films and nanostructures.

Patterning nanorods, nanowires, and nanotubes with good control of their assembly and alignments is also of great interest as building blocks in nanoelectronics and photonics.[99] Again, a general approach is to use surfaces with patterns of contrasting wettability to selectively deposit and align the nanomaterials based on the interactions between the solvent and the patterned surface.[51]

Bao and coworkers controlled the assembly and alignment of palladium nanorods (250 nm diameter, 6 μm length) by depositing palladium nanorod suspensions on surfaces patterned with hydrophobic (1-hexadecanethiol-functionalized gold, $\theta_{st} \approx 98°$) and hydrophilic (bare gold, $\theta_{st} \approx 64°$) regions.[100] After the nanorods were allowed to settle for 10 min, the excess suspension was removed from the substrate using a pipette resulting in small, discrete droplets of the nanorod suspension on the hydrophilic regions. Nanorods could be aligned in hydrophilic regions with widths less than the length of the nanorods by dip-coating the patterned substrate in a nanorod suspension and evaporating the droplets. Using superhydrophilic–superhydrophobic patterned surfaces instead would result in a higher contrast in wettability between the two regions and could allow finer pattern designs

and more precise arrangement of the nanorods, as well as more options in terms of suspension medium and particle properties. Zhang and coworkers implemented a similar approach by using SiO_2 substrates with patterns of wettability to grow or deposit arrays of organic nanowires.[101]

Bao and coworkers demonstrated selective deposition of organic semiconducting crystals onto and between source and drain electrodes to create arrays of single-crystal organic field-effect transistors.[102] Despite their high performance, integrating single crystals into electronic devices is challenging to mass-produce because the single crystals are usually handpicked and placed onto the device substrate, and thus nearly impossible to fabricate devices using submicrometre-sized organic crystals. The method presented by Bao and coworkers was based on solvent wetting and dewetting to assemble organic semiconducting crystals of 5,5′-bis(4-*tert*-butylphenyl)-2,2′-bithiophene (tPTTPt) directly onto transistor source–drain electrodes. A suspension of tPTTPt was allowed to settle on the hydrophilic electrodes for 10 min and then the excess solution was removed from the hydrophobic dielectric layer with a pipette, leaving behind small, discrete droplets of tPTTPt suspension on the electrodes due to discontinuous dewetting. Field-effect transistor behaviour was observed with tPTTPt crystals, but further work is needed to improve the crystal quality and optimize the assembly conditions and contact between the dielectric/semiconductor and electrode/semiconductor.

So far, we have presented how surfaces with wettability patterns could be used to create 1D/2D structures. Song and coworkers were able to use hydrophilic–hydrophobic patterned surfaces to create 3D microstructures.[103] They controlled pinning of a droplet containing nanoparticles at the three-phase contact line (TCL) by tuning the surface energy difference at the interface of hydrophilic and hydrophobic regions as well as the properties of the solution, and promoted asymmetric dewetting to manipulate the droplet morphology (Figure 7.4). For liquid droplets containing nanoparticles, the TCL slides along a surface with low surface energy in a centripetal direction, leading to a dome-like deposition. On a surface with high surface energy, TCL pinning usually occurs and results in a ring-like deposition. 3D colloidal crystals were deposited from a microdroplet onto specially designed hydrophilic pinning patterns fabricated by introducing hydrophilic pinning points (θ_{st} = 58.3° ± 1.5°) onto a homogeneous hydrophobic surface (θ_{st} = 109.4° ± 1.1°). A monodisperse solution of poly(styrene-methyl methacrylate-acrylic acid) nanoparticles (mean diameter = 210 nm) was printed with a commercial inkjet printer so that each droplet covered three hydrophilic pinning points arranged in a triangle. The nanoparticles moved along with the asymmetrically shrinking TCL of the droplets to form 3D triangle-shaped microcolloidal crystals. When the TCL was pinned on the hydrophilic points, capillary flow from the hydrophobic to the hydrophilic regions drove the nanoparticles to the hydrophilic regions and they settled along the curved surface of the droplet. However, the TCL on the hydrophobic background retracted inward but was restrained by the pinning points and resulted in triangular droplet morphologies. This method can be further developed for creating 3D microstructures

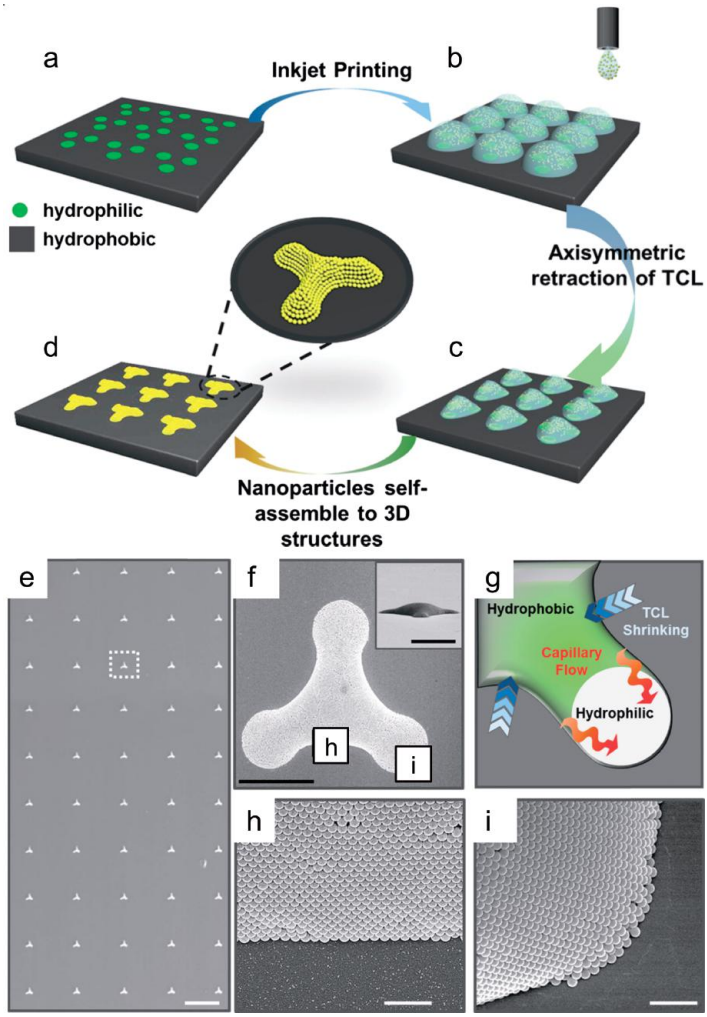

Figure 7.4 (a–d) Schematic of the formation of 3D microcolloidal crystal patterns. (a) A hydrophobic silicon wafer with patterned hydrophilic pinning spots (green) is used as the substrate. (b) Inkjet printing is used to dispense an array of droplets containing nanoparticles at designed locations. (c) An array of triangular droplets is formed by hydrophilic pattern-induced asymmetric dewetting. (d) Arrayed 3D microcolloidal crystals with controllable morphology are achieved. (e–i) Typical morphology of the 3D microcolloidal crystals. (e) SEM image of arrayed microcolloidal crystals. Scale bar is 200 μm. (f) Top-view SEM image of a compactly assembled microcolloidal crystal structure. Inset: Side-view SEM image of the microcolloidal crystal. Scale bars are 20 μm. (g) Schematic of the mechanism of nanoparticle assembly on the hydrophilic region. (h–i) SEM images of the hydrophobic and hydrophilic regions shown in (f). Scale bars are 10 μm. Adapted with permission from John Wiley and Sons ref. 103 Copyright © 2015 Wiley-VCH Verlag GmbH & Co. KGaA, Weinheim.

with other functional materials, such as quantum dots and metal nanoparticles, to achieve suitable defect-free structures for various applications.

7.3.5 Self-Assembly of Microchips

Capillary-driven self-alignment of droplets is a common technique used in microassembly technologies, where the surface tension of a liquid aligns microchips to patterns on the substrate. Zhou and coworkers developed an oleophilic–oleophobic patterned surface and demonstrated the self-alignment of SU-8 (an epoxy-based negative photoresist) microchips using droplets of adhesive (Delo 18507) in ambient air environment.[104] Gold patterns were used to create the oleophilic receptor sites, and a topographical microstructure of porous ormocer functionalized with a fluorinated trichlorosilane was fabricated for the surrounding oleophobic area. The adhesive had a static contact angle of 53° on the oleophilic area, 119° on the oleophobic area, and 47° on the SU-8 chip. Self-assembly of a microchip was demonstrated by moving an SU-8 chip (200 μm × 200 μm × 50 μm) towards a droplet of adhesive (0.5–1.5 nl) dispensed onto a gold receptor site (200 μm × 200 μm), releasing the chip, and then allowing the capillary force to self-align the chip according to the gold pattern (Figure 7.5a–d). Zhou and coworkers later demonstrated self-assembly of microchips, but using hydrophobic receptor sites (silica functionalized with fluoropolymer) patterned on a superhydrophobic surface (nanostructured black silicon surface functionalized with fluoropolymer) and a water droplet as the self-alignment medium.[105]

Zhou and coworkers further demonstrated that capillary self-transport and self-alignment of microchips could still be achieved without requiring any initial overlap between the microchips and the receptor sites.[14] In this case, the surface consisted of hydrophilic silicon receptor sites surrounded by superhydrophobic black silicon coated with a fluoropolymer, and microscopic rain (droplets of 1–5 μm diameter) was used as the medium for capillary self-transport. When a sufficient amount of water droplets rained on the surface, the droplets between the chip and the hydrophilic receptor site grew until a meniscus was established between the chip and the receptor site. This meniscus and the water film on the receptor site coalesced, and the meniscus then reduced its total surface energy by pulling the chip towards and aligning with the hydrophilic receptor site (Figure 7.5e–j). This method of applying microscopic rain on hydrophilic–superhydrophobic patterned surfaces greatly improved the capability, reliability, and error tolerance of the chip self-assembly process.

7.3.6 Lithographic Printing

Lithographic printing uses a chemically patterned surface with anisotropic wetting such that hydrophobic areas accept ink and hydrophilic areas repel ink for reprography. When the plate is introduced to an ink and water mixture, the ink adheres to the hydrophobic graphic areas to be printed while

the water cleans the hydrophilic background. This flat plate can be used directly, or it can be offset by transferring the graphic onto a flexible sheet (*e.g.* rubber) to enable much longer and more detailed print runs. Surfaces with sharply contrasting patterns of hydrophobicity and hydrophilicity are crucial for forming high-resolution images when using printing techniques based on wetting and non-wetting regions.

Fujishima and coworkers used superhydrophilic–superhydrophobic patterned substrates for offset printing by wetting the superhydrophilic regions

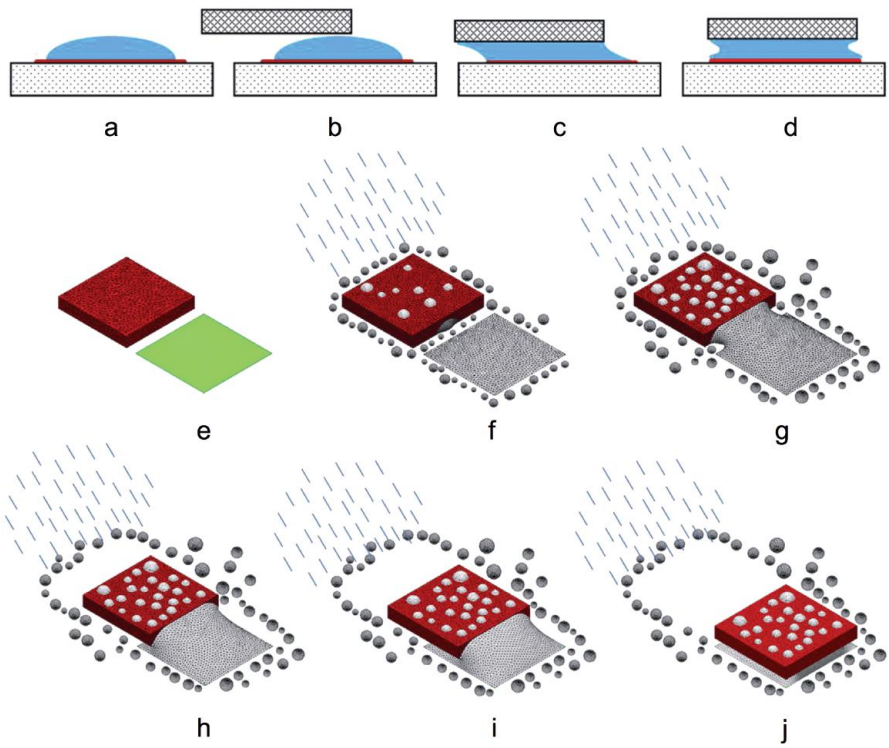

Figure 7.5 (a–d) Schematic of droplet self-alignment. (a) A droplet of liquid is dispensed on a pattern. (b) A chip approaches a pattern with a predefined releasing bias. (c) The droplet wets the chip, and a meniscus is formed between the chip and the pattern. (d) The chip is released and the capillary force aligns the chip to the pattern. Adapted with permission from B. Chang, *et al., Sci. Rep.,* 2015, 5, 14966.[104] Copyright © 2011 AIP Publishing LLC. (e–j) Schematic of capillary self-transport using microscopic rain. (e) A chip (red) is placed outside a receptor site (green) with the same shape and size. (f) Microscopic rain is delivered onto the assembly site and water droplets accumulate on the hydrophilic receptor site and superhydrophobic substrate. (g) A water meniscus is formed between the chip and the receptor site. (h–j) The chip is dragged towards the receptor site and finally aligned with the receptor site. Adapted with permission ref. 14. Copyright © 2015 Nature Publishing Group.

with water and allowing the water-insoluble ink to coat only the superhydrophobic graphic regions.[46] Colour printing at a resolution of 133 lines per inch was achieved. After the print run was complete, the hydrophobic regions could be photocatalytically decomposed by irradiation with UV light to obtain the original superhydrophilic surface for re-patterning with another graphic. A single superhydrophilic–superhydrophobic patterned plate was also able to print 40 000 copies per hour with a web press, demonstrating the robustness of the substrate.

Jiang and coworkers developed a superhydrophobic, photoconductive, aligned ZnO nanorod-array surface that could undergo a controlled transition of the patterned wettability *via* a photoelectric cooperative wetting process.[106] Electrowetting was activated in the direction parallel to the nanorods due to the capillary effect only where the surface was illuminated by white light. The nanorod-array surface was used for liquid reprography by first applying a water-soluble ink such that it exhibited the Cassie–Baxter state on the superhydrophobic surface, and then white light was illuminated on the surface through a photomask to transition the wettability of the ink to the Wenzel state in the desired graphic pattern. After the excess ink was removed from the surface, the ink pattern was then easily transferred to hydrophilic paper to print the reprographic image.

7.3.7 Patterning Textiles

Liu and coworkers treated cotton fabric to create hydrophilic and hydrophobic patterns and demonstrated their use as stamps.[107] Cotton fibres were coated with poly(dimethylsiloxane)-*block*-poly[2-(cinnamoyloxy)ethyl acrylate] (PDMS-*b*-PCEA) micelles with the assumption that the PDMS block would migrate to the polymer–air interface to reduce the surface tension of the coating and the PCEA block would wrap around the fibre to form an underlying layer. Photolysing the cotton fibres with UV light through a photomask crosslinked the PCEA layer around the fibres in the unmasked regions to create a superhydrophobic Cassie–Baxter surface, and then the fibres were rinsed with a solvent to remove the coating from the non-crosslinked regions to regenerate the hydrophilic cotton fibres. This resulted in hydrophilic–superhydrophobic patterned cotton fabrics, which were then attached to the base of a funnel to create stamps for ink printing. Water-based solutions of ink in the funnel permeated the hydrophilic regions, but were blocked by the superhydrophobic regions, so the pattern could be stamped onto a receiving substrate. The pattern was also printed onto cardboard, paper, wood, and aluminium foil.

Pan and coworkers used a different method to create a micropatterned superhydrophobic textile (MST), and demonstrated its potential use for sweat removal.[108] Surface tension-induced pressure gradients produced by extreme differences in wettability as well as capillarity facilitate interfacial microfluidic transport along the fibrous MST. Patterns of hydrophilic yarns were stitched onto a superhydrophobic textile coated with a thin layer of

fluoropolymer microparticles to create a MST. High rates of sweat removal along the hydrophilic yarns were achieved while also maintaining dryness and high gas permittivity through the superhydrophobic textile. A microstitched pattern with five inlets (1 mm diameter) connected by hydrophilic yarn to one outlet (6 mm diameter) was designed for efficient sweat removal by Laplace pressure gradients generated by the curved surface of droplets. This microfluidic transport mechanism on MST is sustainable even during heavy perspiration conditions in humid weather because sweat is continuously transported to the exterior surface and removed by rolling off the superhydrophobic textile. The applications of this interfacial microfluidic transport by MST can be extended to other needs for biofluidic transport, for example removal of urine or collection and drainage of wound exudates.

7.3.8 Patterning Slippery Lubricant-Infused Porous Surfaces

Aizenberg and coworkers recently introduced SLIPS as a water-immiscible fluid, liquid-repellent, durable, defect-free, self-healing interface formed by locking a perfluorinated lubricant within a porous hydrophobic structure.[8] The principle of SLIPS is different from superhydrophobic Cassie–Baxter surfaces in that a fluid–fluid interface between a lubricant and an immiscible liquid is relied upon liquid repellency due to elimination of pinning points and low sliding angles. Since then, there has been much interest in the development of SLIPS for a wide variety applications ranging from anti-biofouling and anti-marine fouling to anti-icing.[109–112]

Many studies on preventing cell adhesion have relied on trapping an air layer within and on top of porous, superhydrophobic surfaces so that liquid on the surface is in the Cassie–Baxter state. However, the cell-repellent properties can diminish after long culture times as the cells grow to confluence and proteins eventually cover the superhydrophobic surface. Despite a lot of research activity in this field, surfaces possessing a combination of (a) efficient cell repellency, (b) long-term stability, and (c) ability to be patterned are still very rare. Ueda and Levkin introduced a newer concept based on SLIPS for patterning cell-repellent regions, which have proven to be more efficient than conventional cell-repellent coatings such as PEG-functionalized surfaces.[25] They developed a method to selectively and precisely pattern SLIPS (hydrophobic liquid) on porous superhydrophilic–superhydrophobic patterned surfaces to efficiently prevent cell adhesion and create cell microarrays.[25] First, a nanoporous polymer surface with superhydrophilic spots separated by superhydrophobic barriers was wetted with water to form droplets in the superhydrophilic spots by discontinuous dewetting (Figure 7.6).[22] Second, a thin layer of hydrophobic liquid (Krytox® GPL 103) was spread over the surface including over the water droplets, but the hydrophobic liquid only penetrated the superhydrophobic barriers. Third, the hydrophobic liquid layer was washed off the superhydrophilic spots, but it did not wash away from the superhydrophobic barriers and formed a stable micropattern on the polymer surface. The hydrophobic liquid barriers confined adherent cell

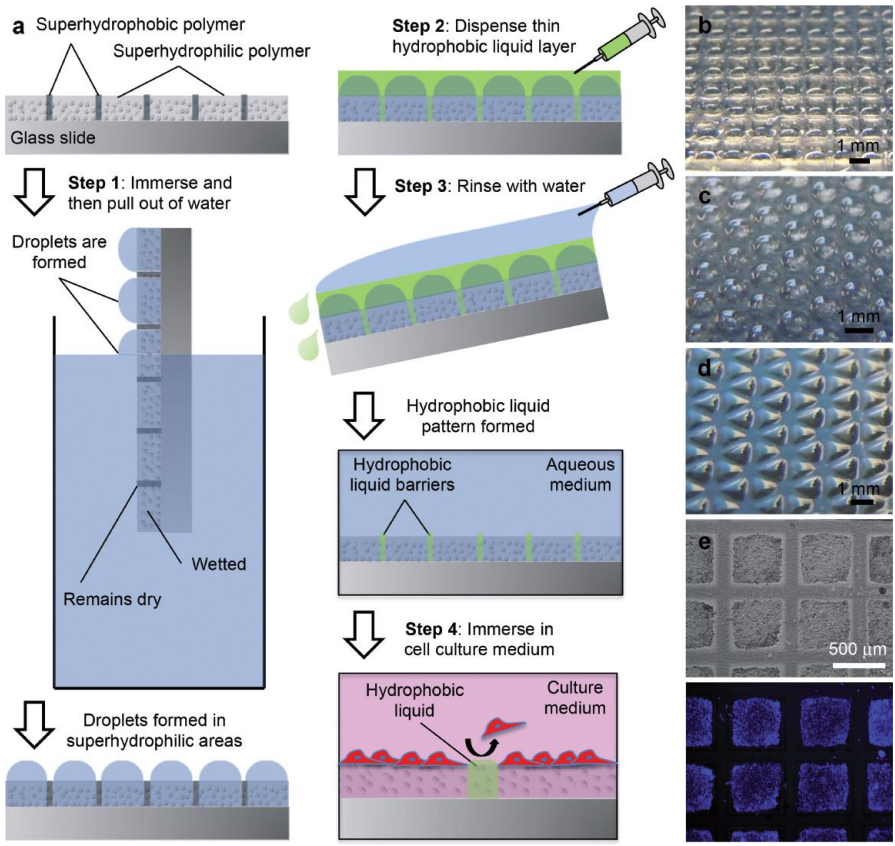

Figure 7.6 (a) Schematic of a superhydrophilic nanoporous polymer surface with superhydrophobic moieties. Step 1: when the superhydrophilic–superhydrophobic patterned substrate is immersed in water, the superhydrophilic areas become easily wetted while the superhydrophobic areas remain dry. When the substrate is pulled out of water, only the superhydrophilic areas remain filled with water and distinct droplets are formed. Step 2: a thin layer of hydrophobic liquid is applied over the water droplets, but infuses only the non-wetted superhydrophobic areas. Step 3: the surface is rinsed with water to wash off the unstable hydrophobic liquid layer covering the water droplets. The hydrophobic liquid infused in the superhydrophobic areas remains stable, resulting in the formation of a hydrophobic liquid pattern. Step 4: cells cultured on hydrophobic liquid patterns adhere to the superhydrophilic areas, but are easily removed from the hydrophobic liquid barriers by weak shear forces. (b–d) Water droplets in superhydrophilic spots separated by 100 µm hydrophobic liquid barriers for different array pattern geometries: (b) 1 mm side length square, (c) 1 mm diameter circle, and (d) 1 mm side length triangle. (e) HEK 293 cells cultured on a hydrophobic liquid micropattern (500 µm side length square, 100 µm barrier). Brightfield and DAPI channel (blue) images are shown. Reproduced with permission from John Wiley and Sons ref. 25. Copyright © 2013 Wiley-VCH Verlag GmbH & Co. KGaA, Weinheim.

types within the superhydrophilic spots, even when the cell population grew to a high density and virtually no cells migrated across the hydrophobic liquid barrier (see Figure 7.6). The few cells that were present on the hydrophobic liquid barriers after 7 days of culture displayed a rounder morphology compared with cells on the superhydrophilic spots and were easily removed by shear forces when gently washing the substrate. This suggested that the cells did not readily adhere and grow on the hydrophobic liquid, but no cytotoxic effects were observed. The slippery, water-immiscible, and self-healing nature of the stable hydrophobic liquid layer formed on the porous surfaces most likely attributed to the cell-resistant behaviour due to the inability of the cells to become anchored to the liquid interface.[8,109] The hydrophobic liquid micropatterns were stable and demonstrated long-term repellent properties against eukaryotic cells, which surpassed that of a PEG-functionalized surface.

Vogel *et al.* also later demonstrated that Krytox® 100 lubricant could be patterned on a substrate and could be used to spatially confine a variety of fluids, including low surface tension liquids or biological fluids.[113]

Lee and coworkers developed a micro-omnifluidic (μ-OF) system based on a phenomenon called microchannel induction that spontaneously occurs when droplets of solvents are applied on omniphilic micropatterned regions of a SLIPS.[114] Photolithography was used to create 2D omniphilic paths on rough fluorinated surfaces, and then the substrates were infused with lubricant. The μ-OF system was compatible with all solvents tested that had a surface tension greater than that of the lubricant used (here, Fluorinert™ FC-70, 17.1 mN m^{-1}) and all solvents that were also able to repel the infused lubricant and settle on the omniphilic micropatterns. Gravity triggered the controlled movement of droplets, which were guided by the induced 2D omniphilic microchannels. The μ-OF system was also designed for mixing droplets using a Y-shaped omniphilic pattern (60 μm line width) with a large omniphilic square patch (200 μm side length) at the Y-junction for droplet mixing. This μ-OF device does not require a pump and is compatible with almost any solvent. Although poly(dimethylsiloxane) (PDMS) microchannels are widely used, one critical issue is the incompatibility of PDMS with organic solvents. Thus, the μ-OF system has potential to be used for microfluidic channels when working with organic solvents or other harsh chemicals.

Manna and Lynn designed SLIPS by infusing silicone oil into nanoporous, hydrophobic polymer multilayers fabricated by reactive or covalent layer-by-layer assembly.[115] The reactivity of the azlactone-functionalized multilayers provided a means to tune the surface and bulk wetting behaviours by treatment with amine-functionalized molecules. The multilayers were chemically patterned with hydrophilic D-glucamine followed by functionalization of the background with 1-decylamine, and then infused with oil. Sticky regions devoid of oil were obtained that could stop the sliding of aqueous liquids, extract samples of liquid, and control the trajectories of sliding droplets. These SLIPS-coated surfaces patterned with sticky patches captured droplets from aqueous dye solutions by dip-coating. If the droplets are large enough

compared with the spacing between sticky patches, then the velocity and trajectory of the droplets can be controlled.

Since SLIPS have also demonstrated to be effective against fouling from bacteria, marine organisms, and ice, patterned SLIPS could be useful for applications, for example, in the medical, marine, and transportation industries to design sophisticated anti-fouling surfaces.[109–112]

7.3.9 Fog Collection

Jiang and coworkers combined both wettability and shape gradients for more efficient water collection compared with simple circle-shaped wettability patterns or uniform superhydrophilic or superhydrophobic surfaces.[116] Star-shaped wettability patterns were designed to integrate surface energy gradients and Laplace pressure gradients to quickly drive tiny water droplets towards more wettable regions (Figure 7.7). Reducing the pattern size further improved the water collection efficiency. Highly porous superhydrophilic surfaces (~19.2 μm thick, $\theta_{st} \approx 0°$) were fabricated by spin-coating a TiO_2 slurry onto a bare glass substrate, and then superhydrophobic surfaces ($\theta_{st} > 150°$) could be fabricated by treating the superhydrophilic surface with heptadecafluorodecyl-trimethoxysilane (FAS). Superhydrophilic patterns ($\theta_{st} < 5°$) in the shape of circles or 4-, 5-, 6-, and 8-pointed stars were created by exposure of FAS-modified superhydrophobic surface to UV light (365 nm, ~25 mW cm^{-2}) for 60 min through a photomask to photocatalytically decompose the FAS monolayer in the exposed regions.

The water collection properties from a flow of fog generated by a humidifier (relative humidity >95%) were tested on four kinds of surfaces: uniformly superhydrophilic, uniformly superhydrophobic, circle-patterned, and eight-pointed star-patterned. Droplets spread immediately when captured on the uniformly superhydrophilic surfaces, whereas droplets maintained a spherical shape and frequently coalesced with neighbouring droplets on the uniformly superhydrophobic surfaces. On the circular patterns, droplets were mostly collected and easily coalesced on the outer superhydrophobic region and then were driven inward to the wettable circular region by the gradient in surface energy. Actually capturing the water droplets from the air is a crucial step for efficient water collection, thus an eight-pointed star-shaped pattern was designed to capture tiny water droplets, quickly let them coalesce into larger droplets before they evaporate, and transport them to a reservoir. On the eight-pointed star-shaped patterned surface, droplets were initially captured everywhere on the surface but were then driven by the gradient in surface energy from the outer superhydrophobic region to the superhydrophilic star pattern to form larger droplets. Furthermore, the tips of the star generated a Laplace pressure gradient due to the shape gradient and further enhanced the directional movement of water droplets. Surfaces with the star-shaped pattern were more efficient at collecting water than the circular patterns (2.11 *vs.* 2.78 g cm^{-2} h^{-1}). These experiments indicate that gradients in surface energy

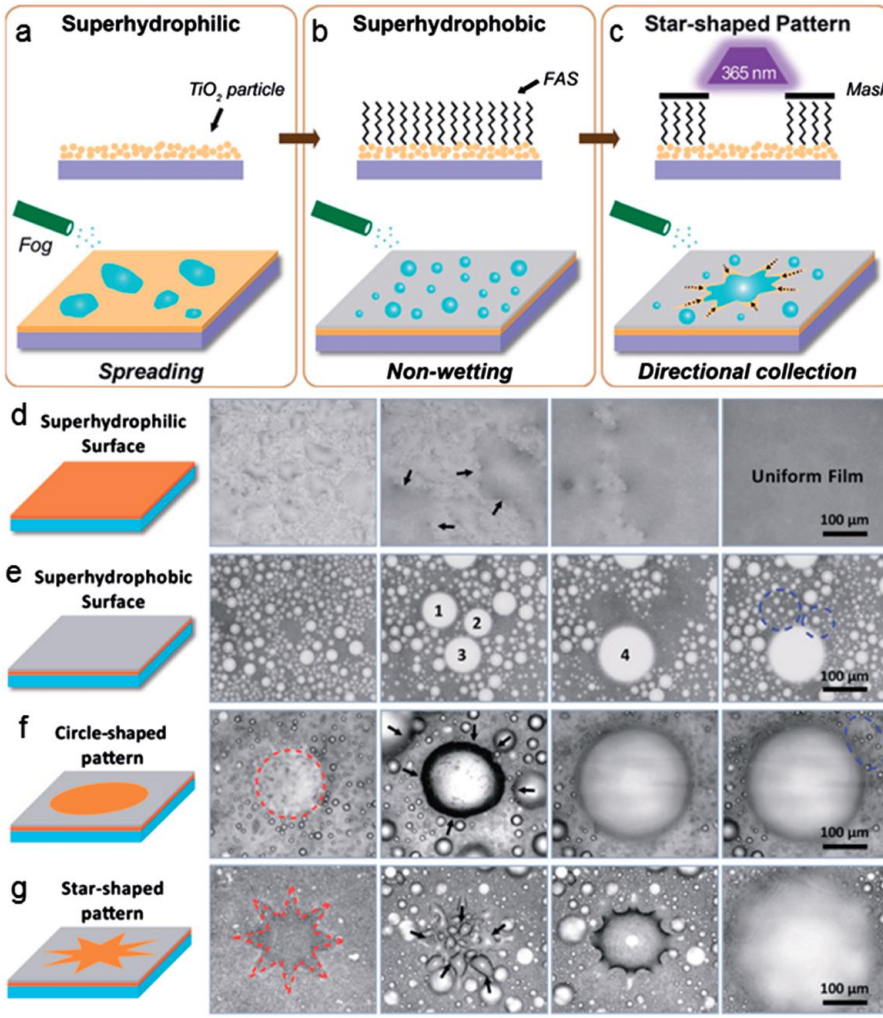

Figure 7.7 Schematic of the fabrication of surfaces with different wettabilities. (a) Superhydrophilic surface composed of TiO_2 nanoparticles, where fog droplets spread. (b) Superhydrophobic surface modified with heptadecafluorodecyl-trimethoxysilane (FAS) showing a non-wetting property to fog droplets. (c) Bioinspired gradient surface with a star-shaped wettability pattern fabricated by illuminating the FAS-modified film through a photomask with UV light. The fog droplets are collected directionally towards the star-shaped region, which is more wettable. (d–g) Water collection from fog on surfaces with various wettability features. (d) On a uniformly superhydrophilic surface, water droplets spread over surface. (e) On a uniformly superhydrophobic surface, individual water droplets coalesce randomly (*e.g.* droplet 1 + 2 + 3 to 4). (f, g) On surfaces with patterns of wettability, tiny water droplets are collected directionally toward the more wettable region (indicated by the arrows). The water collecting processes are continuous because new droplets appear immediately after the previous ones move away, which enhances the fog-collecting efficiency. Adapted with permission from John Wiley and Sons ref. 116. Copyright © 2014 Wiley-VCH Verlag GmbH & Co. KGaA, Weinheim.

and shape as well as the size of the superhydrophilic patterns influence the water collection efficiency. Surfaces patterned with similar but smaller shapes were more efficient at collecting water than those with a larger pattern because the Laplace pressure gradient is highly sensitive to the length scale.

Wang and coworkers used superhydrophilic–superhydrophobic micropatterned surfaces to demonstrate enhanced efficiency of water collection from fog compared with uniform superhydrophilic and superhydrophobic surfaces.[43] The patterned surfaces were fabricated by inkjet printing a dopamine solution in a designated pattern onto a superhydrophobic surface, followed by *in situ* dopamine polymerization to create superhydrophilic regions. For the water collection experiments, the substrates were placed on a thermoelectric cooling module to maintain the substrates at ~4 °C, which is lower than the dew point of 20 °C, and a simulated flow of fog (~10 cm s^{-1}) was generated by a humidifier. The temperature and relative humidity were approximately 22 °C and 90–95%, respectively. The substrates were vertically oriented and the water collected by the surfaces drained by gravity into containers underneath the substrates. The weight of water collected was measured after 1 h for five different substrates: a superhydrophilic glass substrate with $\theta_{st} < 5°$; a superhydrophobic glass substrate; and PDA-patterned superhydrophobic substrates with pattern sizes/separations of either 200 μm/400 μm, 200 μm/1000 μm, or 500 μm/1000 μm. The superhydrophilic surface had the lowest water collection efficiency (~14.9 mg cm^{-2} h^{-1}) among the five different substrates. The superhydrophobic surface reached a water collection efficiency of ~30.0 mg cm^{-2} h^{-1}; however, all three PDA-patterned superhydrophobic surfaces demonstrated even more enhanced water collection efficiency ranging from ~33.2 to 61.8 mg cm^{-2} h^{-1}, with the 500 μm/1000 μm pattern design achieving the highest efficiency.

On the superhydrophilic surface, film-wise condensation occurred in that the condensed water droplets immediately spread on the surface and formed a thin water film. On the superhydrophobic surface, tiny spherical water droplets condensed on the surface and gradually merged into larger droplets until reaching a threshold and rolling off the vertical surface. Self-clearing of the droplets from the superhydrophobic surface allowed continuous nucleation and growth of new droplets, resulting in more efficient collection of water. On the PDA-patterned superhydrophobic surfaces, condensation of tiny water droplets occurred initially on the superhydrophobic regions, but then the droplets preferentially moved towards the PDA-modified superhydrophilic regions due to the difference in wettability and subsequently coalesced into bigger droplets in these regions until reaching a threshold and rolling off the surface. The superhydrophilic–superhydrophobic patterned surfaces were seemingly more efficient at collecting water from fog due to the simultaneous enhancement of droplet nucleation on the superhydrophilic regions along with droplet removal on the superhydrophobic regions.

7.3.10 Heat Transfer During Boiling

Tuteja and coworkers developed superomniphobic–superomniphilic patterned surfaces to improve the heat transfer for more efficient boiling with both aqueous and non-aqueous liquids with low surface tension (*e.g.* oil, alcohol).[44] Surfaces with low surface energy are not easily wetted by boiling liquid and exhibit a high boiling heat transfer coefficient because they facilitate bubble nucleation. Superomniphobic surfaces yield high heat transfer coefficient values even for low surface tension, heat transfer liquids. When the critical heat flux is reached during boiling, the rate of bubble nucleation increases until finally the bubbles coalesce to form a continuous vapour film between the heated surface and the boiling liquid. This vapour film has a high thermal resistance and acts as a barrier to heat transfer. Patterned superomniphobic–superomniphilic surfaces increase the heat transfer coefficient and critical heat flux even more since the superomniphobic regions promote high nucleation rates, while the superomniphilic regions help to prevent the formation of a continuous vapour film. Heptane preferentially condensed within patterned superomniphilic regions and methanol preferentially boiled on patterned superomniphobic regions.

7.4 Conclusions

Research involving surfaces patterned with extreme differences in wettability is actively progressing. A variety of different techniques to produce patterned surfaces have already been developed, but there is still room to improve the robustness, stability, and ease of fabrication and modification of such surfaces. More importantly, novel and practical applications of patterned surfaces are still being developed. In this chapter, we have introduced some of the applications that have been utilized for patterned surfaces: STCM devices for separation or liquid control applications; using superhydrophobic regions in the Cassie–Baxter state to control protein and cell adhesion as well as cell migration; creating ultrahigh-density cell or droplet arrays; controlling the shape and positioning of liquid droplets or microparticles; patterning ink for lithographic printing; patterning hydrophobic lubricants for highly efficient cell repellency; efficient water collection and droplet transport in low moisture conditions; and improved nucleation of bubbles and heat transfer during boiling.

Since the adhesion of molecules and cells was well controlled by patterns of superhydrophobicity in the Cassie–Baxter state, it is an interesting alternative to using physical barriers for applications such as cell patterning, cell screening using microarrays, performing bioassays, controlling the adhesion of biomolecules and cells in complex 2D or 3D architectures, tissue engineering, bioimplants, or performing high-throughput combinatorial chemical screens. Using layers of air trapped on the surface is a more general method for controlling protein and cell adhesion since interactions with the surface are minimized and seem to be mostly independent of the protein structure

or chemical composition. In addition, protein and cell repellence would not rely on serum-free or serum-depleted conditions.

Culturing cells in arrays of droplets or hydrogels opens up the possibilities of screening non-adherent cells and cells in 3D microenvironments. In addition to demonstrating the cell-repellent properties of superhydrophobic surfaces, we showed that hydrophobic lubricant surfaces also possess excellent and long-term cell-repellent properties. The concept of hydrophobic lubricant-infused porous surfaces for anti-biofouling applications has recently been introduced, but the mechanism of cell repellency has not been confirmed and should be explored in detail. This information could lead to the better design of non-fouling surfaces. In the near future, surfaces with patterns of wettability will be further implemented to advance the performance and potential of existing or new technologies.

Acknowledgements

The authors are grateful to the European Research Council (ERC Starting Grant, DropCellArray 337077) for the financial support.

References

1. A. R. Parker and C. R. Lawrence, *Nature*, 2001, **414**, 33.
2. L. Zhai, M. C. Berg, F. C. Cebeci, Y. Kim, J. M. Milwid, M. F. Rubner and R. E. Cohen, *Nano Lett.*, 2006, **6**, 1213.
3. R. P. Garrod, L. G. Harris, W. C. E. Schofield, J. McGettrick, L. J. Ward, D. O. H. Teare and J. P. S. Badyal, *Langmuir*, 2007, **23**, 689.
4. C. Dorrer and J. Rühe, *Langmuir*, 2008, **24**, 6154.
5. D. Ishii, H. Yabu and M. Shimomura, *Chem. Mater.*, 2009, **21**, 1799.
6. S. C. Thickett, C. Neto and A. T. Harris, *Adv. Mater.*, 2011, **23**, 3718.
7. C.-P. Hsu, Y.-M. Lin and P.-Y. Chen, *JOM*, 2015, **67**, 744.
8. T.-S. Wong, S. H. Kang, S. K. Y. Tang, E. J. Smythe, B. D. Hatton, A. Grinthal and J. Aizenberg, *Nature*, 2011, **477**, 443.
9. T. Ishizaki, N. Saito and O. Takai, *Langmuir*, 2010, **26**, 8147.
10. N. M. Oliveira, A. I. Neto, W. Song and J. F. Mano, *Appl. Phys. Express*, 2010, **3**, 1.
11. S. M. Oliveira, W. Song, N. M. Alves and J. F. Mano, *Soft Matter*, 2011, **7**, 8932.
12. A. I. Neto, C. A. Custódio, W. Song and J. F. Mano, *Soft Matter*, 2011, **7**, 4147.
13. C. L. Salgado, M. B. Oliveira and J. F. Mano, *Integr. Biol.*, 2012, **4**, 318.
14. B. Chang, A. Shah, Q. Zhou, R. H. A. Ras and K. Hjort, *Sci. Rep.*, 2015, **5**, 14966.
15. L. Sainiemi, V. Jokinen, A. Shah, M. Shpak, S. Aura, P. Suvanto and S. Franssila, *Adv. Mater.*, 2011, **23**, 122.
16. N. M. Alves, I. Pashkuleva, R. L. Reis and J. F. Mano, *Small*, 2010, **6**, 2208.
17. F. Svec, *J. Chromatogr., A*, 2010, **1217**, 902.

18. P. A. Levkin, F. Svec and J. M. J. Fréchet, *Adv. Funct. Mater.*, 2009, **19**, 1993.
19. Y. Han, P. Levkin, I. Abarientos, H. Liu, F. Svec and J. M. J. Fréchet, *Anal. Chem.*, 2010, **82**, 2520.
20. D. Zahner, J. Abagat, F. Svec, J. M. J. Fréchet and P. A. Levkin, *Adv. Mater.*, 2011, **23**, 3030.
21. F. L. Geyer, E. Ueda, U. Liebel, N. Grau and P. A. Levkin, *Angew. Chem., Int. Ed.*, 2011, **50**, 8424.
22. E. Ueda, F. L. Geyer, V. Nedashkivska and P. A. Levkin, *Lab Chip*, 2012, **12**, 5218.
23. A. N. Efremov, E. Stanganello, A. Welle, S. Scholpp and P. A. Levkin, *Biomaterials*, 2012, **34**, 1757.
24. P. Auad, E. Ueda and P. A. Levkin, *ACS Appl. Mater. Interfaces*, 2013, **5**, 8053.
25. E. Ueda and P. A. Levkin, *Adv. Healthcare Mater.*, 2013, **2**, 1425.
26. K. Kreppenhofer, J. Li, R. Segura, L. Popp, M. Rossi, P. Tzvetkova, B. Luy, C. J. Kähler, A. E. Guber and P. A. Levkin, *Langmuir*, 2013, **29**, 3797.
27. A. N. Efremov, M. Grunze and P. A. Levkin, *Adv. Mater. Interfaces*, 2014, **1**, 1.
28. R. M. Hensarling, V. A. Doughty, J. W. Chan and D. L. Patton, *J. Am. Chem. Soc.*, 2009, **131**, 14673.
29. W. Feng, L. Li, E. Ueda, J. Li, S. Heißler, A. Welle, O. Trapp and P. A. Levkin, *Adv. Mater. Interfaces*, 2014, **1**, 1.
30. J. Li, L. Li, X. Du, W. Feng, A. Welle, O. Trapp, M. Grunze, M. Hirtz and P. A. Levkin, *Nano Lett.*, 2015, **15**, 675.
31. W. Feng, L. Li, C. Yang, A. Welle, O. Trapp and P. A. Levkin, *Angew. Chem., Int. Ed.*, 2015, **54**, 8732.
32. H. Lee, S. M. Dellatore, W. M. Miller and P. B. Messersmith, *Science*, 2007, **318**, 426.
33. H. O. Ham, Z. Liu, K. H. A. Lau, H. Lee and P. B. Messersmith, *Angew. Chem., Int. Ed.*, 2011, **50**, 732.
34. B. P. Lee, P. B. Messersmith, J. N. Israelachvili and J. H. Waite, *Annu. Rev. Mater. Res.*, 2011, **41**, 99.
35. K. Chawla, S. Lee, B. P. Lee, J. L. Dalsin, P. B. Messersmith and N. D. Spencer, *J. Biomed. Mater. Res., Part A*, 2009, **90**, 742.
36. S. M. Kang, N. S. Hwang, J. Yeom, S. Y. Park, P. B. Messersmith, I. S. Choi, R. Langer, D. G. Anderson and H. Lee, *Adv. Funct. Mater.*, 2012, **22**, 2949.
37. C. Rodriguez-Emmenegger, C. M. Preuss, B. Yameen, O. Pop-Georgievski, M. Bachmann, J. O. Mueller, M. Bruns, A. S. Goldmann, M. Bastmeyer and C. Barner-Kowollik, *Adv. Mater.*, 2013, **25**, 6123.
38. L. Zhang, H. Yu, N. Zhao, Z.-M. Dang and J. Xu, *J. Appl. Polym. Sci.*, 2014, **131**, 1.
39. X. Du, L. Li, J. Li, C. Yang, N. Frenkel, A. Welle, S. Heissler, A. Nefedov, M. Grunze and P. A. Levkin, *Adv. Mater.*, 2014, **26**, 8029.
40. J. Sedó, J. Saiz-Poseu, F. Busqué and D. Ruiz-Molina, *Adv. Mater.*, 2013, **25**, 653.

41. Y. Liu, K. Ai and L. Lu, *Chem. Rev.*, 2014, **114**, 5057.
42. S. M. Kang, I. You, W. K. Cho, H. K. Shon, T. G. Lee, I. S. Choi, J. M. Karp and H. Lee, *Angew. Chem., Int. Ed.*, 2010, **49**, 9401.
43. L. Zhang, J. Wu, M. N. Hedhili, X. Yang and P. Wang, *J. Mater. Chem. A*, 2015, **3**, 2844.
44. S. P. R. Kobaku, A. K. Kota, D. H. Lee, J. M. Mabry and A. Tuteja, *Angew. Chem., Int. Ed.*, 2012, **51**, 10109.
45. U. Manna, A. H. Broderick and D. M. Lynn, *Adv. Mater.*, 2012, **24**, 4291.
46. S. Nishimoto, A. Kubo, K. Nohara, X. Zhang, N. Taneichi, T. Okui, Z. Liu, K. Nakata, H. Sakai, T. Murakami, M. Abe, T. Komine and A. Fujishima, *Appl. Surf. Sci.*, 2009, **255**, 6221.
47. Y. Lai, F. Pan, C. Xu, H. Fuchs and L. Chi, *Adv. Mater.*, 2013, **25**, 1682.
48. J. S. Li, E. Ueda, A. Nallapaneni, L. X. Li and P. A. Levkin, *Langmuir*, 2012, **28**, 8286.
49. G. Arrabito and B. Pignataro, *Anal. Chem.*, 2012, **84**, 5450.
50. I. P. Parkin, L. Wang, S. Huang, J. Song, Y. Lu, W. Xu, F. Chen and X. Liu, *Micro Nano Lett.*, 2015, **10**, 105.
51. L. Wen, Y. Tian and L. Jiang, *Angew. Chem., Int. Ed.*, 2015, **54**, 3387.
52. I. You, N. Yun and H. Lee, *ChemPhysChem*, 2013, **14**, 471.
53. M. J. Hancock, J. He, J. F. Mano and A. Khademhosseini, *Small*, 2011, **7**, 892.
54. M. J. Hancock, F. Yanagawa, Y. Jang, J. He, N. N. Kachouie, H. Kaji and A. Khademhosseini, *Small*, 2012, **8**, 393.
55. M. J. Hancock, F. Piraino, G. Camci-Unal, M. Rasponi and A. Khademhosseini, *Biomaterials*, 2011, **32**, 6493.
56. F. Piraino, G. Camci-Unal, M. J. Hancock, M. Rasponi and A. Khademhosseini, *Lab Chip*, 2012, **12**, 659.
57. X. Liu, Q. Wang, J. Qin and B. Lin, *Lab Chip*, 2009, **9**, 1200.
58. I. You, S. M. Kang, S. Lee, Y. O. Cho, J. B. Kim, S. B. Lee, Y. S. Nam and H. Lee, *Angew. Chem., Int. Ed.*, 2012, **51**, 6126.
59. A. B. D. Cassie and S. Baxter, *Trans. Faraday Soc.*, 1944, **40**, 546.
60. T. Koishi, K. Yasuoka, S. Fujikawa, T. Ebisuzaki and X. C. Zeng, *Proc. Natl. Acad. Sci.*, 2009, **106**, 8435.
61. J. Ballester-Beltrán, P. Rico, D. Moratal, W. Song, J. F. Mano and M. Salmerón-Sánchez, *Soft Matter*, 2011, **7**, 10803.
62. L. Baugh and V. Vogel, *J. Biomed. Mater. Res., Part A*, 2004, **69**, 525.
63. J. Ziauddin and D. M. Sabatini, *Nature*, 2001, **411**, 107.
64. H. Erfle, B. Neumann, U. Liebel, P. Rogers, M. Held, T. Walter, J. Ellenberg and R. Pepperkok, *Nat. Protoc.*, 2007, **2**, 392.
65. M. Stürzl, A. Konrad, G. Sander, E. Wies, F. Neipel, E. Naschberger, S. Reipschläger, N. Gonin-Laurent, R. E. Horch, U. Kneser, W. Hohenberger, H. Erfle and M. Thurau, *Comb. Chem. High Throughput Screening*, 2008, **11**, 159.
66. J. K. Rantala, R. Mäkelä, A.-R. Aaltola, P. Laasola, J.-P. Mpindi, M. Nees, P. Saviranta and O. Kallioniemi, *BMC Genomics*, 2011, **12**, 1.
67. E. Palmer, *Methods Mol. Biol.*, 2011, **706**, 1.
68. K. Papp, Z. Szittner and J. Prechl, *Cell. Mol. Life Sci.*, 2012, **69**, 2717.

69. K. C. Wood, D. J. Konieczkowski, C. M. Johannessen, J. S. Boehm, P. Tamayo, O. B. Botvinnik, J. P. Mesirov, W. C. Hahn, D. E. Root, L. A. Garraway and D. M. Sabatini, *Sci. Signaling*, 2012, **5**, 1.
70. R. Onuki-Nagasaki, A. Nagasaki, K. Hakamada, T. Q. Uyeda, M. Miyake, J. Miyake and S. Fujita, *BMC Genet.*, 2015, **16**, 1.
71. M. Buchholz, T. Honstein, S. Kirchhoff, R. Kreider, H. Schmidt, B. Sipos and T. M. Gress, *PLoS One*, 2015, **10**, 1.
72. H. M. Botelho, I. Uliyakina, N. T. Awatade, M. C. Proença, C. Tischer, L. Sirianant, K. Kunzelmann, R. Pepperkok and M. D. Amaral, *Sci. Rep.*, 2015, **5**, 1.
73. A. Revzin, R. G. Tompkins and M. Toner, *Langmuir*, 2003, **19**, 9855.
74. H. Ma, D. Li, X. Sheng, B. Zhao and A. Chilkoti, *Langmuir*, 2006, **22**, 3751.
75. A. L. Hook, H. Thissen and N. H. Voelcker, *Biomacromolecules*, 2009, **10**, 573.
76. S. Fujita, R. Onuki-Nagasaki, J. Fukuda, J. Enomoto, S. Yamaguchi and M. Miyake, *Lab Chip*, 2012, **13**, 77.
77. M. R. Carstens, R. C. Fisher, A. P. Acharya, E. A. Butterworth, E. Scott, E. H. Huang and B. G. Keselowsky, *Proc. Natl. Acad. Sci.*, 2015, **112**, 8732.
78. Y. Arima and H. Iwata, *Biomaterials*, 2007, **28**, 3074.
79. S. Mousses, N. J. Caplen, R. Cornelison, D. Weaver, M. Basik, S. Hautaniemi, A. G. Elkahloun, R. A. Lotufo, A. Choudary, E. R. Dougherty, E. Suh and O. Kallioniemi, *Genome Res.*, 2003, **13**, 2341.
80. S. Baghdoyan, Y. Roupioz, A. Pitaval, D. Castel, E. Khomyakova, A. Papine, F. Soussaline and X. Gidrol, *Nucleic Acids Res.*, 2004, **32**, 1.
81. B. Neumann, M. Held, U. Liebel, H. Erfle, P. Rogers, R. Pepperkok and J. Ellenberg, *Nat. Methods*, 2006, **3**, 385.
82. B. N. Lourenço, G. Marchioli, W. Song, R. L. Reis, C. A. van Blitterswijk, M. Karperien, A. van Apeldoorn and J. F. Mano, *Biointerphases*, 2012, **7**, 1.
83. B. Schaack, J. Reboud, S. Combe, B. Fouqué, F. Berger, S. Boccard, O. Filhol-Cochet and F. Chatelain, *NanoBiotechnology*, 2005, **1**, 183.
84. A. J. You, R. J. Jackman, G. M. Whitesides and S. L. Schreiber, *Chem. Biol.*, 1997, **4**, 969.
85. R. J. Jackman, D. C. Duffy, E. Ostuni, N. D. Willmore and G. M. Whitesides, *Anal. Chem.*, 1998, **70**, 2280.
86. J. H. Butler, M. Cronin, K. M. Anderson, G. M. Biddison, F. Chatelain, M. Cummer, D. J. Davi, L. Fisher, A. W. Frauendorf, F. W. Frueh, C. Gjerstad, T. F. Harper, S. D. Kernahan, D. Q. Long, M. Pho, J. A. Walker and T. M. Brennan, *J. Am. Chem. Soc.*, 2001, **123**, 8887.
87. Y. Xia, Y. Yin, Y. Lu and J. McLellan, *Adv. Funct. Mater.*, 2003, **13**, 907.
88. L. Jongpaiboonkit, W. J. King and W. L. Murphy, *Tissue Eng., Part A*, 2009, **15**, 343.
89. J. W. Nichol, S. T. Koshy, H. Bae, C. M. Hwang, S. Yamanlar and A. Khademhosseini, *Biomaterials*, 2010, **31**, 5536.
90. A. A. Popova, S. M. Schillo, K. Demir, E. Ueda, A. Nesterov-Mueller and P. A. Levkin, *Adv. Mater.*, 2015, **27**, 5217.

91. M. W. Tibbitt and K. S. Anseth, *Biotechnol. Bioeng.*, 2009, **103**, 655.
92. C. A. DeForest and K. S. Anseth, *Annu. Rev. Chem. Biomol. Eng.*, 2012, **3**, 421.
93. P. Lei, R. M. Padmashali and S. T. Andreadis, *Biomaterials*, 2009, **30**, 3790.
94. L. Mugherli, O. N. Burchak, L. A. Balakireva, A. Thomas, F. Chatelain and M. Y. Balakirev, *Angew. Chem., Int. Ed.*, 2009, **48**, 7639.
95. O. N. Burchak, L. Mugherli, M. Ostuni, J. J. Lacapère and M. Y. Balakirev, *J. Am. Chem. Soc.*, 2011, **133**, 10058.
96. W. Feng, L. Li, X. Du, A. Welle and P. A. Levkin, *Adv. Mater.*, 2016, **28**, 3202.
97. F. Fan and K. J. Stebe, *Langmuir*, 2005, **21**, 1149.
98. C. L. Wirth, M. De Volder and J. Vermant, *Langmuir*, 2015, **31**, 1632.
99. S.-Y. Zhang, M. D. Regulacio and M.-Y. Han, *Chem. Soc. Rev.*, 2014, **43**, 2301.
100. S. Liu, J. B.-H. Tok, J. Locklin and Z. Bao, *Small*, 2006, **2**, 1448.
101. R.-R. Bao, C.-Y. Zhang, X.-J. Zhang, X.-M. Ou, C.-S. Lee, J.-S. Jie and X.-H. Zhang, *ACS Appl. Mater. Interfaces*, 2013, **5**, 5757.
102. S. Liu, W. M. Wang, S. C. B. Mannsfeld, J. Locklin, P. Erk, M. Gomez, F. Richter and Z. Bao, *Langmuir*, 2007, **23**, 7428.
103. L. Wu, Z. Dong, M. Kuang, Y. Li, F. Li, L. Jiang and Y. Song, *Adv. Funct. Mater.*, 2015, **25**, 2237.
104. B. Chang, V. Sariola, S. Aura, R. H. A. Ras, M. Klonner, H. Lipsanen and Q. Zhou, *Appl. Phys. Lett.*, 2011, **99**, 1.
105. B. Chang, A. Shah, I. Routa, H. Lipsanen and Q. Zhou, *Appl. Phys. Lett.*, 2012, **101**, 1.
106. D. Tian, Q. Chen, F.-Q. Nie, J. Xu, Y. Song and L. Jiang, *Adv. Mater.*, 2009, **21**, 3744.
107. Y. Wang, X. Li, H. Hu, G. Liu and M. Rabnawaz, *J. Mater. Chem. A*, 2014, **2**, 8094.
108. S. Xing, J. Jiang and T. Pan, *Lab Chip*, 2013, **13**, 1937.
109. A. K. Epstein, T.-S. Wong, R. A. Belisle, E. M. Boggs and J. Aizenberg, *Proc. Natl. Acad. Sci.*, 2012, **109**, 13182.
110. J. Li, T. Kleintschek, A. Rieder, Y. Cheng, T. Baumbach, U. Obst, T. Schwartz and P. A. Levkin, *ACS Appl. Mater. Interfaces*, 2013, **5**, 6704.
111. L. Xiao, J. Li, S. Mieszkin, A. Di Fino, A. S. Clare, M. E. Callow, J. A. Callow, M. Grunze, A. Rosenhahn and P. A. Levkin, *ACS Appl. Mater. Interfaces*, 2013, **5**, 10074.
112. P. Kim, T.-S. Wong, J. Alvarenga, M. J. Kreder, W. E. Adorno-Martinez and J. Aizenberg, *ACS Nano*, 2012, **6**, 6569.
113. N. Vogel, R. A. Belisle, B. Hatton, T.-S. Wong and J. Aizenberg, *Nat. Commun.*, 2013, **4**, 1.
114. I. You, T. G. Lee, Y. S. Nam and H. Lee, *ACS Nano*, 2014, **8**, 9016.
115. U. Manna and D. M. Lynn, *Adv. Mater.*, 2015, **27**, 3007.
116. H. Bai, L. Wang, J. Ju, R. Sun, Y. Zheng and L. Jiang, *Adv. Mater.*, 2014, **26**, 5025.